Streaming Instability and Pebble Accretion: Evidence from the Kuiper Belt

Wladimir Lyra

New Mexico State University

PFITS+

Manuel Cañas (New Mexico State University)**, Daniel Carrera** (New Mexico State University), **Anders Johansen** (University of Copenhagen)**, Leonardo Krapp** (University of Arizona)**, Debanjan Sengupta** (New Mexico State University)**, Jake Simon** (Iowa State University)**, Orkan Umurhan** (NASA Ames)**, Chao-Chin Yang** (University of Alabama)**, Andrew Youdin** (University of Arizona)**.**

Workshop on ISM, Stars, and Planets – Nagoya, Japan – Mar 27th, 2025

The Planetary Science Journal, 5:55 (17pp), 2024 February https://doi.org/10.3847/PSJ/ad1d5b

A Solution for the Density Dichotomy Problem of Kuiper Belt Objects with Multispecies Streaming Instability and Pebble Accretion

Manuel H. Cañas[1], Wladimir Lyra[1], Daniel Carrera[2], Leonardo Krapp[3,7], Debanjan Sengupta[1], Jacob B. Simon[2], Orkan M. Umurhan[4], Chao-Chin Yang (楊朝欽)[5], and Andrew N. Youdin[3,6]
[1] New Mexico State University, Department of Astronomy, P.O. Box 30001 MSC 4500, Las Cruces, NM 88001, USA; wlyra@nmsu.edu
[2] Department of Physics and Astronomy, Iowa State University, Ames, IA 50010, USA
[3] Department of Astronomy and Steward Observatory, University of Arizona, Tucson, AZ 85721, USA
[4] NASA Ames Research Center, Space Sciences Division, Planetary Sciences Branch, Moffatt Field, CA 94035, USA
[5] Department of Physics and Astronomy, University of Alabama, Box 870324, Tuscaloosa, AL 35487-0324, USA
[6] The Lunar and Planetary Laboratory, University of Arizona, Tucson, AZ 85721, USA
Received 2023 August 25; revised 2023 December 27; accepted 2024 January 5; published 2024 February 28

Abstract

Kuiper Belt objects (KBOs) show an unexpected trend, whereby large bodies have increasingly higher densities, up to five times greater than their smaller counterparts. Current explanations for this trend assume formation at constant composition, with the increasing density resulting from gravitational compaction. However, this scenario poses a timing problem to avoid early melting by decay of ^{26}Al. We aim to explain the density trend in the context of streaming instability and pebble accretion. Small pebbles experience lofting into the atmosphere of the disk, being exposed to UV and partially losing their ice via desorption. Conversely, larger pebbles are shielded and remain icier. We use a shearing box model including gas and solids, the latter split into ices and silicate pebbles. Self-gravity is included, allowing dense clumps to collapse into planetesimals. We find that the streaming instability leads to the formation of mostly icy planetesimals, albeit with an unexpected trend that the lighter ones are more silicate-rich than the heavier ones. We feed the resulting planetesimals into a pebble accretion integrator with a continuous size distribution, finding that they undergo drastic changes in composition as they preferentially accrete silicate pebbles. The density and masses of large KBOs are best reproduced if they form between 15 and 22 au. Our solution avoids the timing problem because the first planetesimals are primarily icy and ^{26}Al is mostly incorporated in the slow phase of silicate pebble accretion. Our results lend further credibility to the streaming instability and pebble accretion as formation and growth mechanisms.

Unified Astronomy Thesaurus concepts: Dwarf planets (419); Kuiper Belt (893); Pluto (1267); Hydrodynamics (1963); Planet formation (1241)


Manny Cañas
MSc - NMSU


Wlad Lyra
NMSU


Daniel Carrera
ISU -> NMSU


Leo Krapp
U Arizona


Debanjan Sengupta
NMSU


Jake Simon
ISU

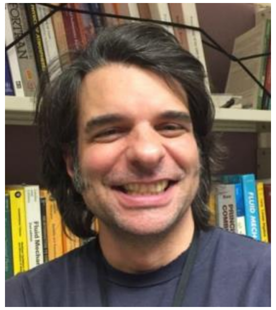
Orkan Umurhan
NASA Ames


Chao-Chin Yang
U Alabama


Andrew Youdin
U Arizona

The Astrophysical Journal, 946:60 (14pp), 2023 April 1 https://doi.org/10.3847/1538-4357/acaf5b

An Analytical Theory for the Growth from Planetesimals to Planets by Polydisperse Pebble Accretion

Wladimir Lyra[1], Anders Johansen[2,3], Manuel H. Cañas[1], and Chao-Chin Yang (楊朝欽)[4]
[1] New Mexico State University, Department of Astronomy, PO Box 30001 MSC 4500, Las Cruces, NM 88001, USA; wlyra@nmsu.edu
[2] Center for Star and Planet Formation, GLOBE Institute, University of Copenhagen, Øster Voldgade 5–7, D-1350 Copenhagen, Denmark
[3] Lund Observatory, Department of Astronomy and Theoretical Physics, Lund University, Box 43, SE-221 00 Lund, Sweden
[4] Department of Physics and Astronomy, University of Alabama, Box 870324, Tuscaloosa, AL 35487-0324, USA
Received 2022 September 6; revised 2022 December 19; accepted 2022 December 29; published 2023 March 30

Abstract

Pebble accretion is recognized as a significant accelerator of planet formation. Yet only formulae for single-sized (monodisperse) distribution have been derived in the literature. These can lead to significant underestimates for Bondi accretion, for which the best accreted pebble size may not be the one that dominates the mass distribution. We derive in this paper the polydisperse theory of pebble accretion. We consider a power-law distribution in pebble radius, and we find the resulting surface and volume number density distribution functions. We derive also the exact monodisperse analytical pebble accretion rate for which 3D accretion and 2D accretion are limits. In addition, we find analytical solutions to the polydisperse 2D Hill and 3D Bondi limits. We integrate the polydisperse pebble accretion numerically for the MRN distribution, finding a slight decrease (by an exact factor 3/7) in the Hill regime compared to the monodisperse case. In contrast, in the Bondi regime, we find accretion rates 1–2 orders of magnitude higher compared to monodisperse, also extending the onset of pebble accretion to 1–2 orders of magnitude lower in mass. We find megayear timescales, within the disk lifetime, for Bondi accretion on top of planetary seeds of masses 10^{-6} to 10^{-4} $M_\oplus$, over a significant range of the parameter space. This mass range overlaps with the high-mass end of the planetesimal initial mass function, and thus pebble accretion is possible directly following formation by streaming instability. This alleviates the need for mutual planetesimal collisions as a major contribution to planetary growth.

Unified Astronomy Thesaurus concepts: Planet formation (1241); Planetary system formation (1257)


Wlad Lyra
NMSU


Anders Johansen
U Copenhagen


Manny Cañas
MSc - NMSU


Chao-Chin Yang
U Alabama

The PFITS+ Collaboration
(Planet Formation in the Southwest)

Co-PIs

Wladimir Lyra – *New Mexico State University*
Andrew Youdin – *University of Arizona*
Jake Simon – *Iowa State University*
Chao-Chin Yang –*University of Alabama*
Orkan Umurhan – *NASA Ames*

Postdocs / Staff

Debanjan Sengupta (NMSU)
Daniel Carrera (ISU -> NMSU)
Sergei Dyda (U Al)
Tabassum Tanvir (ISU)

Graduate Students

NMSU - Daniel Godines, Olivia Brouillette,
Eleanor Serviss, Leopold Hutnik
ISU – Jeonghoon (Jay) Lim, David Rea, Weston Hall
UNLV – Stanley Baronett
U Az – Eonho Chang

Alumni

Manny Cañas (MSc NMSU), Aleksey Mohov (MSc UNLV),
Leonardo Krapp (UAz -> Chile),

The size-density relationship of Kuiper Belt objects

THE ASTROPHYSICAL JOURNAL LETTERS, 778:L34 (

THE DENSITY OF MID-SIZED KUIPER BELT OBJECT 2002 UX25 AND THE FORMATION OF THE DWARF PLANETS

M. E. BROWN
Division of Geological and Planetary Sciences, California Institute of Technology, Pasadena, CA 91125, USA; mbrown@caltech.edu
Received 2013 July 10; accepted 2013 October 28; published 2013 November 13

ABSTRACT

The inferred low rock fraction of the 2002 UX25 system makes the formation of rock-rich larger objects difficult to explain in any standard coagulation scenario. For example, to create an object with the volume of Eris would require assembling ~40 objects of the size of 2002 UX25. Yet the assembled object, even with the additional compression, would still have a density close to 1 g cm^{-3} rather than the 2.5 g cm^{-3} density of Eris (Sicardy et al. 2011).

- Extremely low porosity;
- Biased sample;
- Compaction through giant impacts

None of these alternatives appears likely. We are left in the uncomfortable state of having no satisfying mechanism to explain the formation of the icy dwarf planets. While objects up to the size of 2002 UX25 can easily be formed through standard coagulation scenarios, the rock-rich larger bodies may require a formation mechanism separate from the rest of the Kuiper belt.

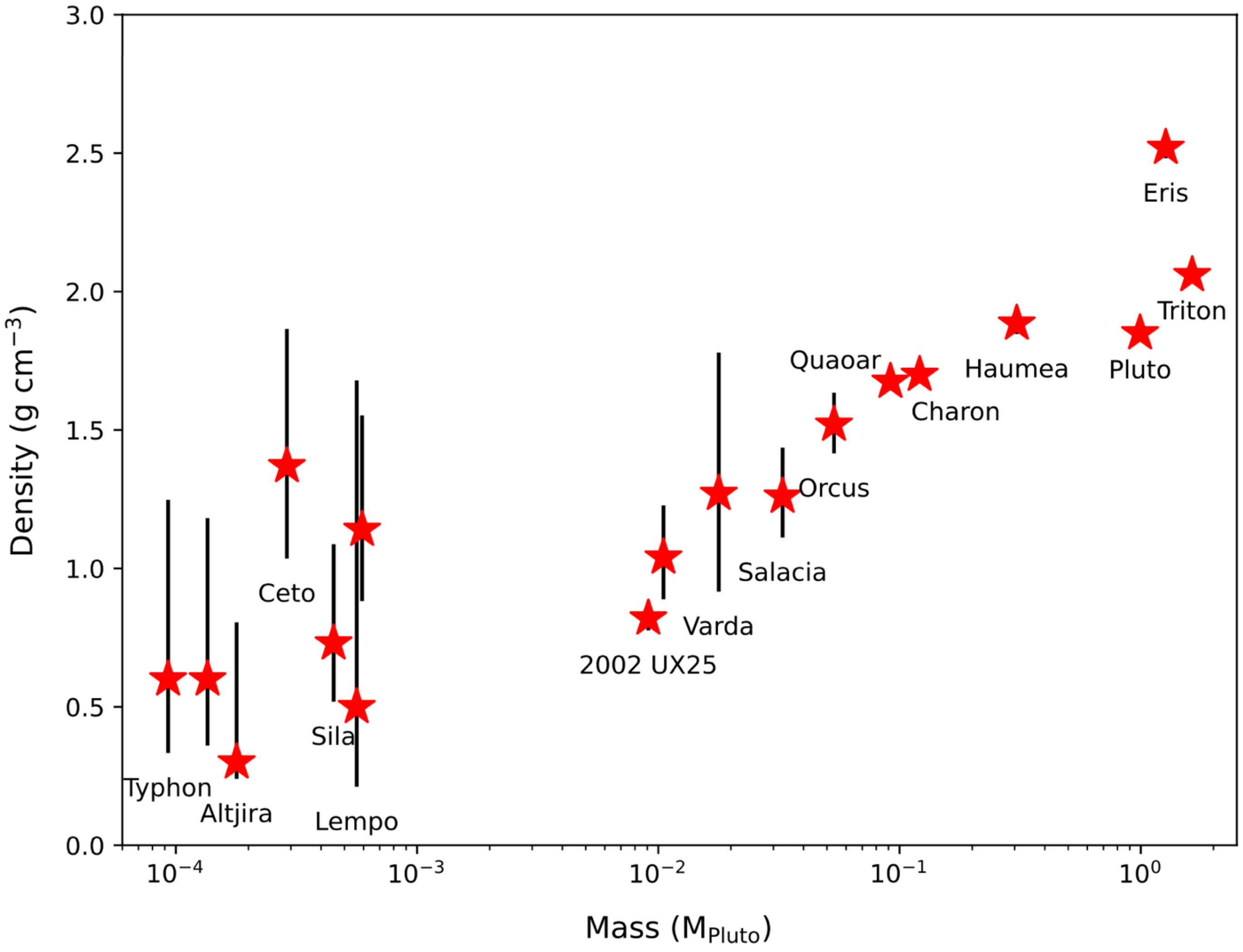

Cañas+Lyra et al. (2024)

Data; *Thomas (2000), Stansberry et al. (2006), Grundy et al. (2007), Brown et al. (2011), Stansberry et al. (2012), Brown (2013), Fornasier et al. (2013), Vilenius, et al. (2014), Nimmo et al. (2016), Ortiz et al. (2017), Brown and Butler (2017), Grundy et al. (2019), Morgado et al. (2023), Pereira et al. (2023).*

Previous best bet:
Porosity removal by gravitational compaction

Problem

- Timing! ^{26}Al would melt if formed within 4 Myr

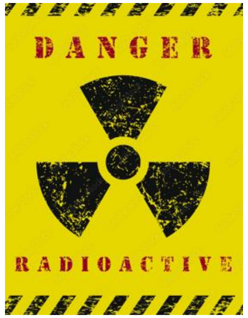

Assumptions

- ~~Constant composition at birth and growth~~
- ~~Growth by planetesimal accretion~~

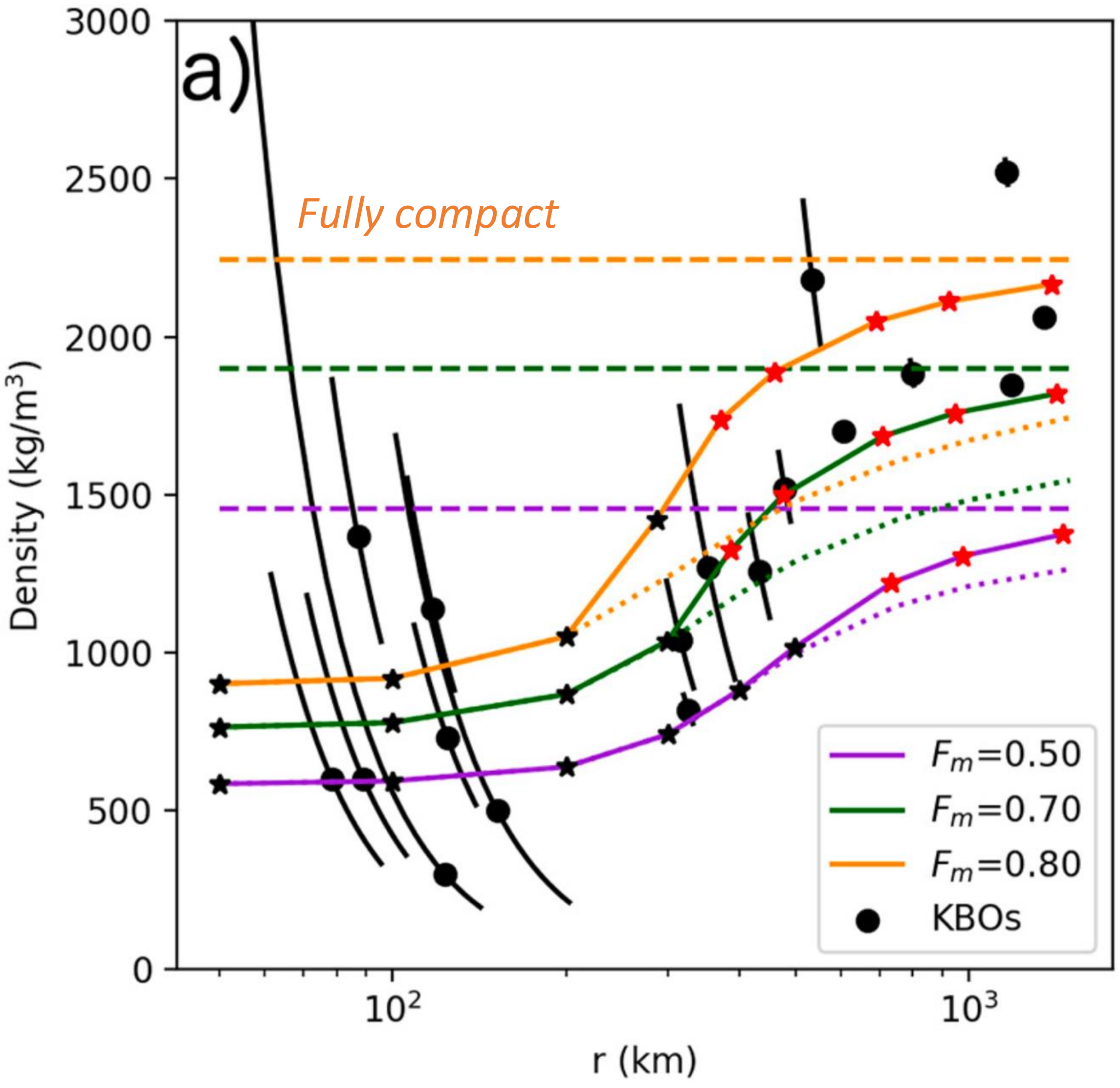

F_m = rock mass fraction

Bierson & Nimmo (2019)

Abandoning Constant Composition

Heating and UV irradiation remove ice on Myr timescales (Harrison & Schoen 1967)

- Small grains lofted in the atmosphere lose ice
- Big grains are shielded and remain icy.

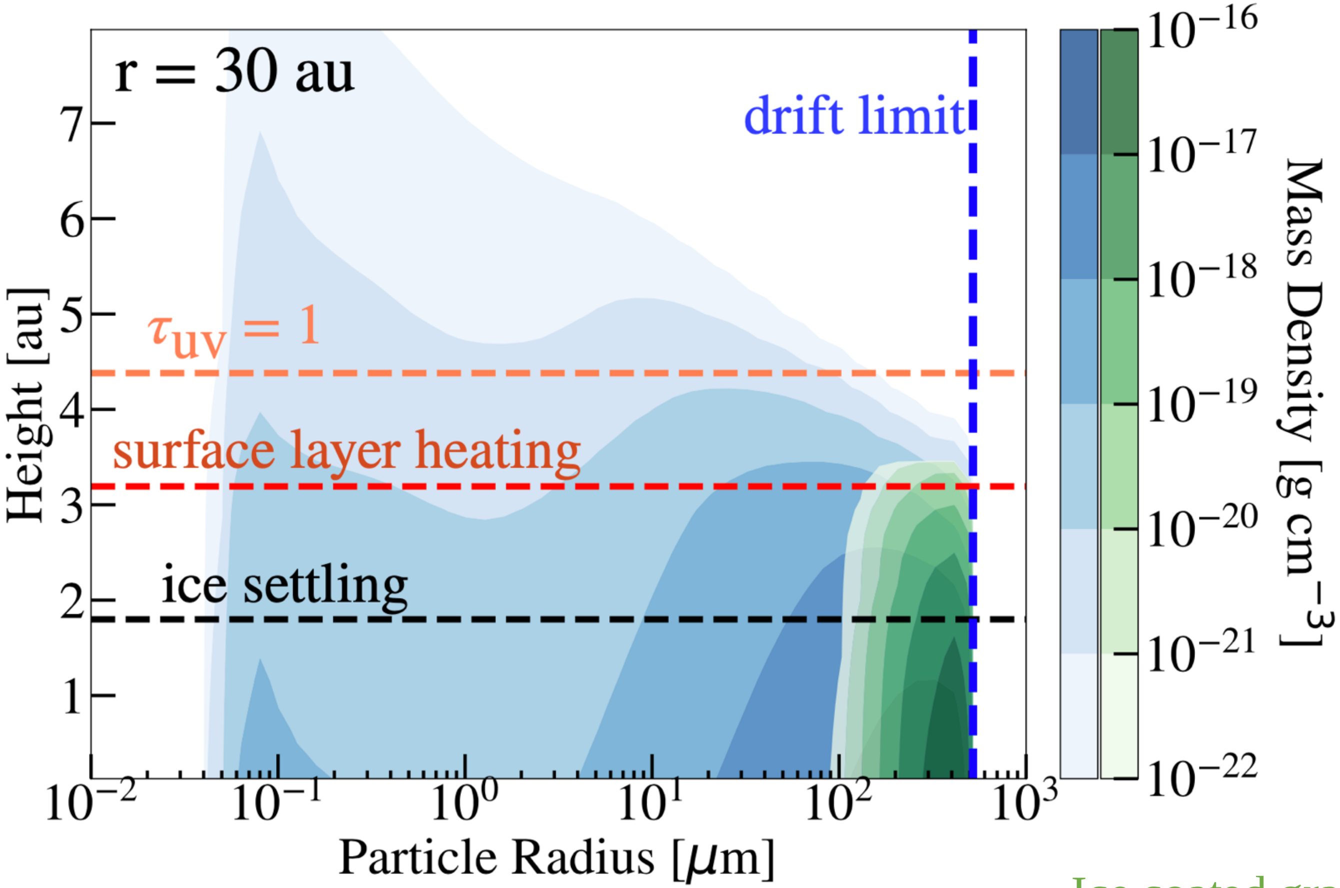

Ice coated grains
Ice-free grains

Powell et al. 2022

Split into icy and silicate pebbles

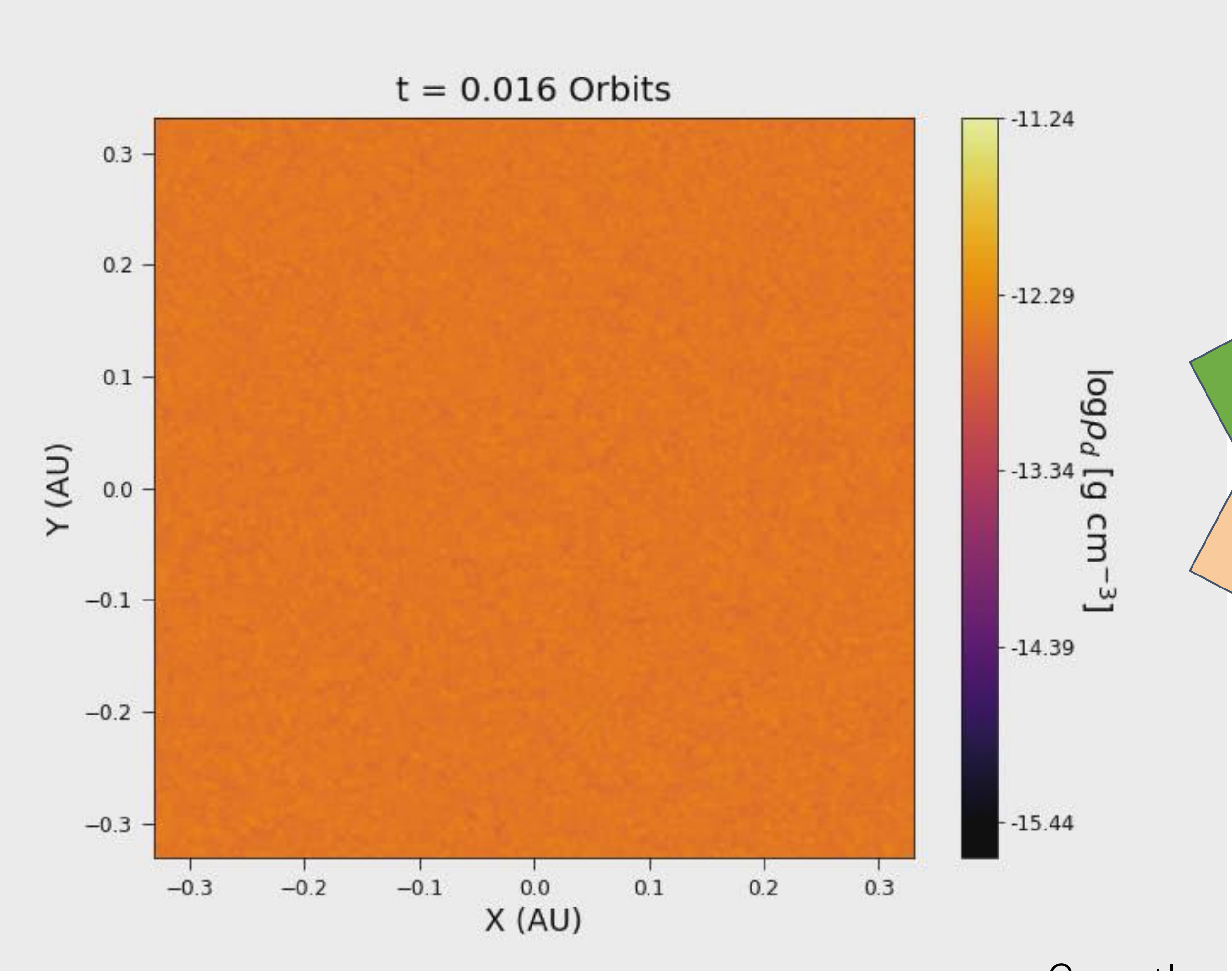

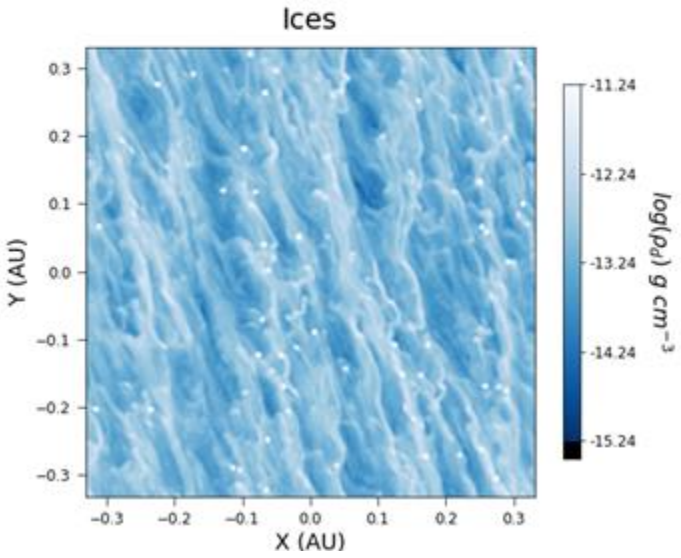

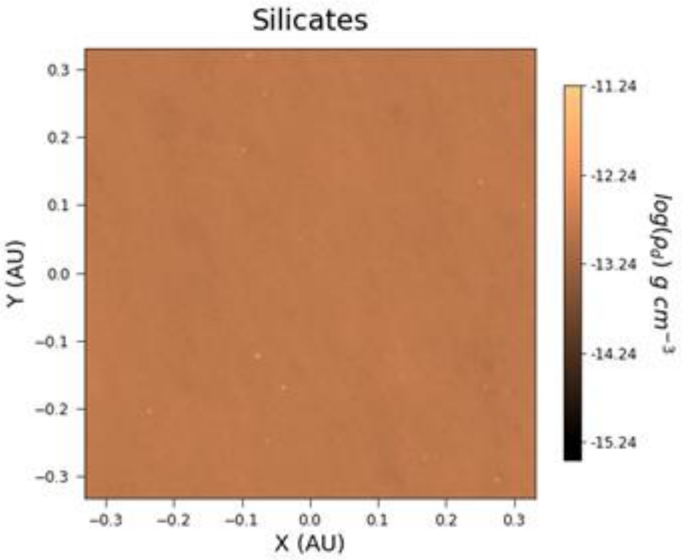

Canas+Lyra et al. 2024

The first planetesimals are icy

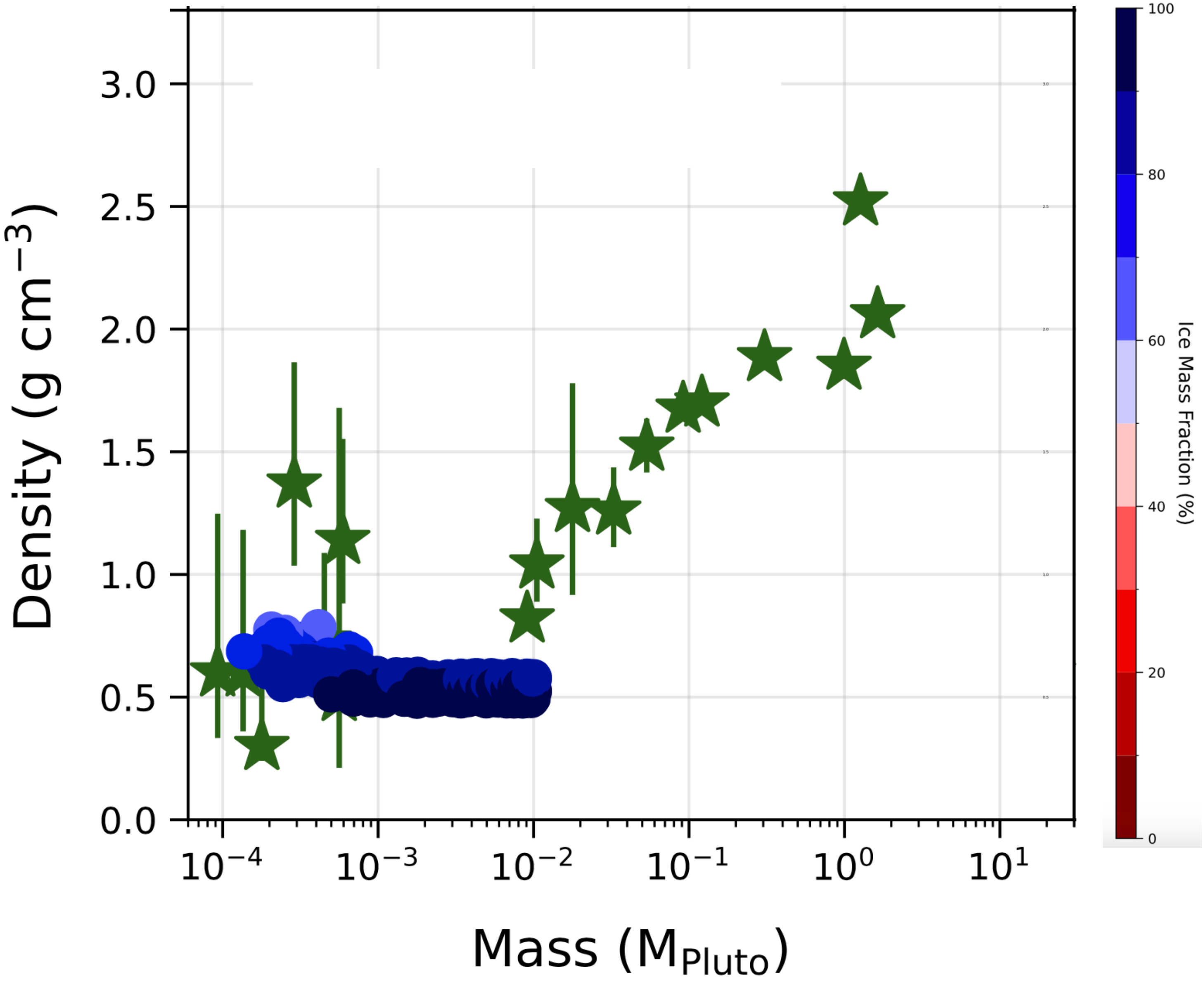

Canas+Lyra et al. 2024

The first planetesimals won't melt

$$\mathcal{H} = \rho\, F_s\, [^{26}\mathrm{Al}]_0\, \mathcal{H}_0\, e^{-\lambda t}$$

$$Q(t) = V \int_0^t \mathcal{H}(t')dt'$$

$$= M_p\, F_s\, [^{26}\mathrm{Al}]_0\, \mathcal{H}_0\, \lambda^{-1} \left(1 - e^{-\lambda t}\right)$$

$$Q = M_p\, c_p\, \Delta T$$

$$\Delta T = F_s\, [^{26}\mathrm{Al}]_0\, \mathcal{H}_0\, \lambda^{-1}\, c_p^{-1}$$

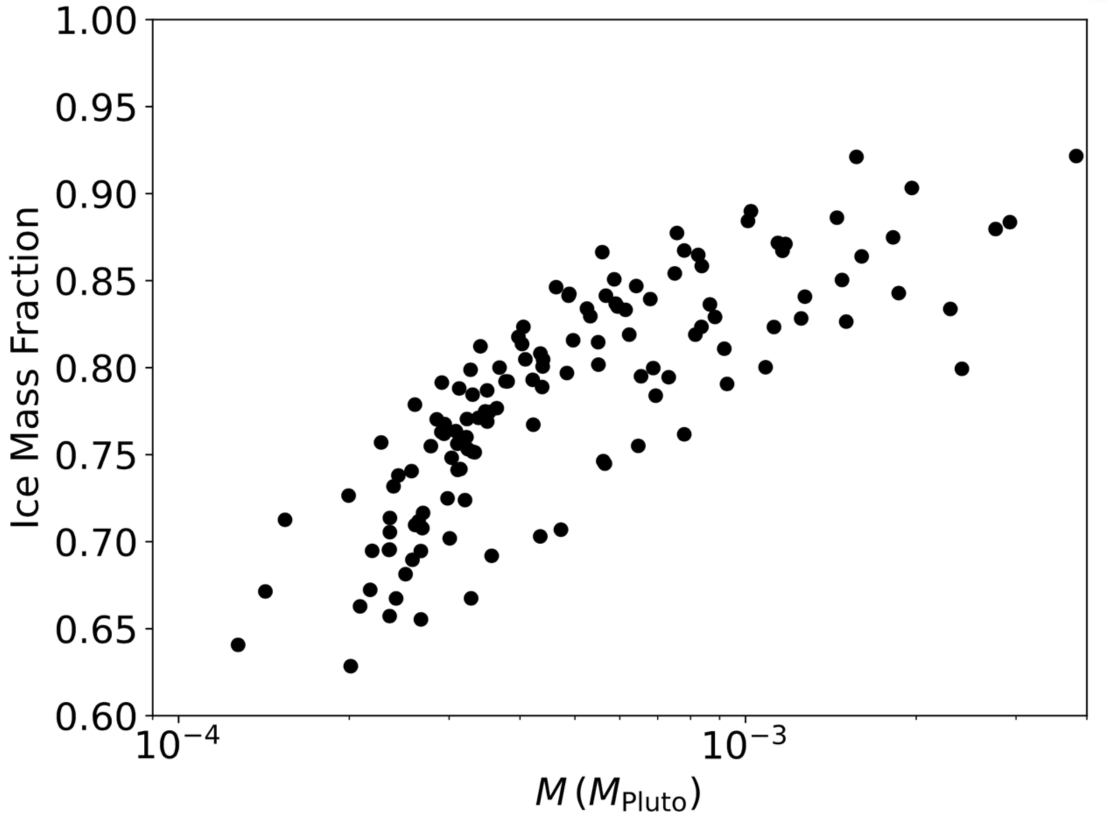

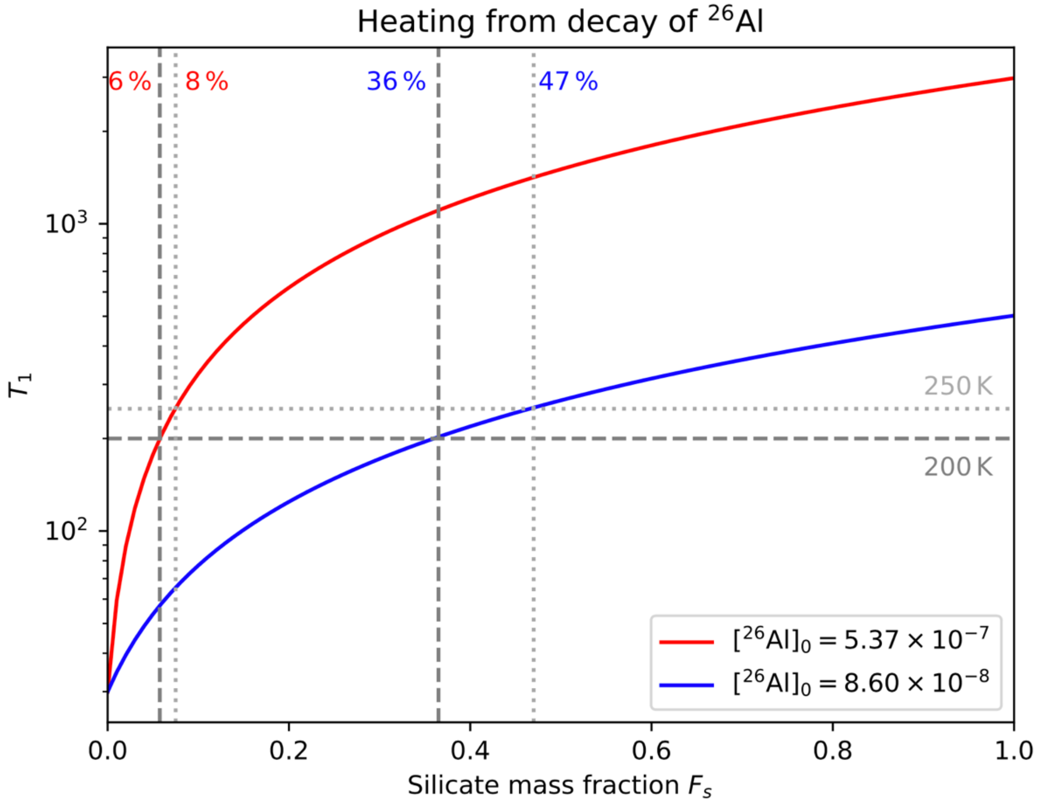

Canas+Lyra et al. 2024

Pebble Accretion: Geometric, Bondi, and Hill regime

Bondi accretion - Bound against headwind

Hill accretion - Bound against stellar tide

$$\xi \equiv \left(\frac{R_{\rm acc}}{2H_d}\right)^2 \qquad \dot{M}_{\rm 3D} = \lim_{\xi\to 0} \dot{M} = \pi R_{\rm acc}^2 \rho_{d0}\delta v, \qquad \dot{M}_{\rm 2D} = \lim_{\xi\to\infty} \dot{M} = 2R_{\rm acc}\Sigma_d \delta v,$$

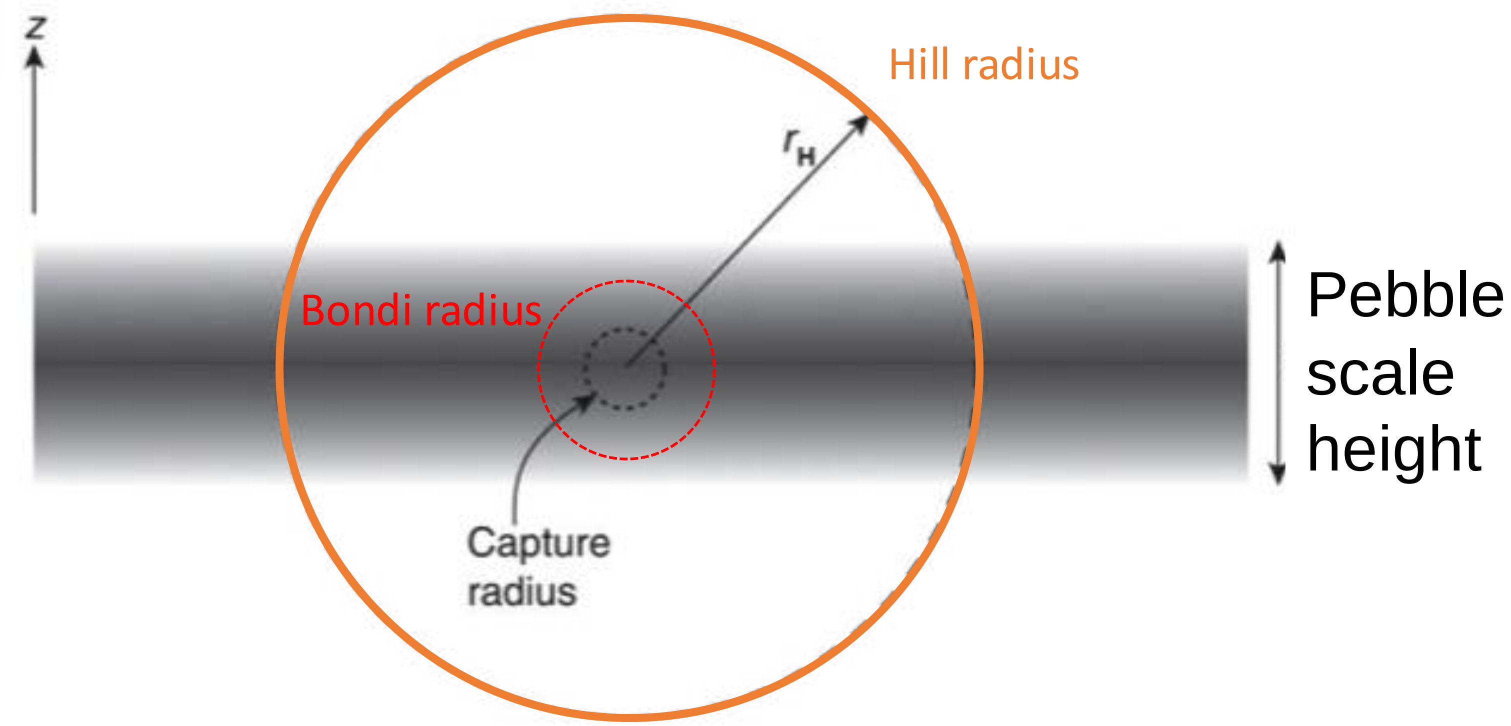

Mass Accretion rates

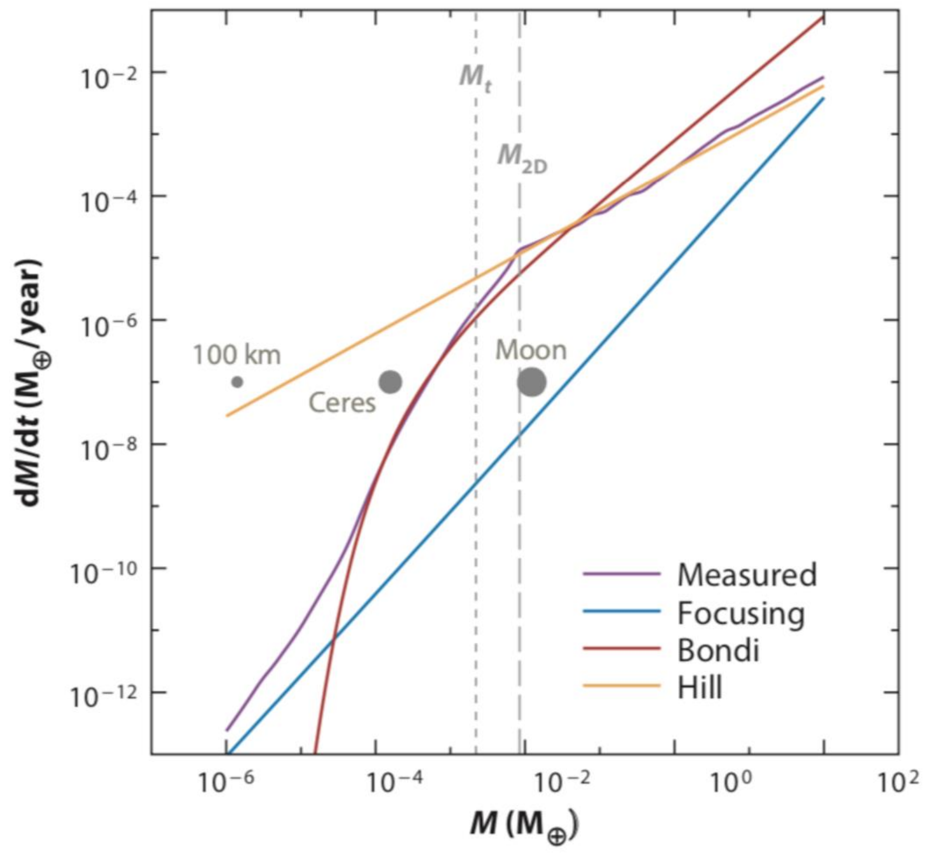

Johansen & Lambrechts '17

Integrate pebble accretion

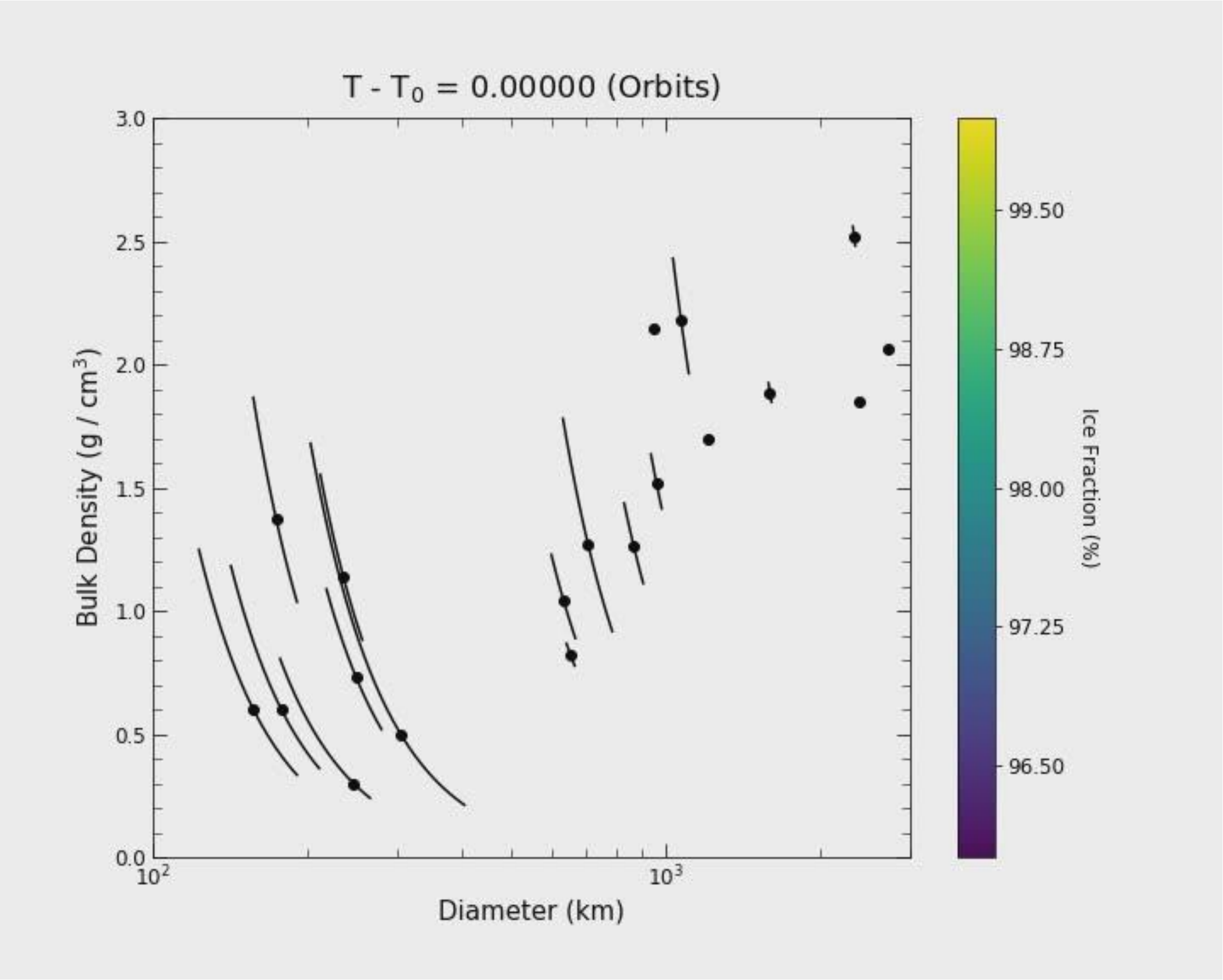

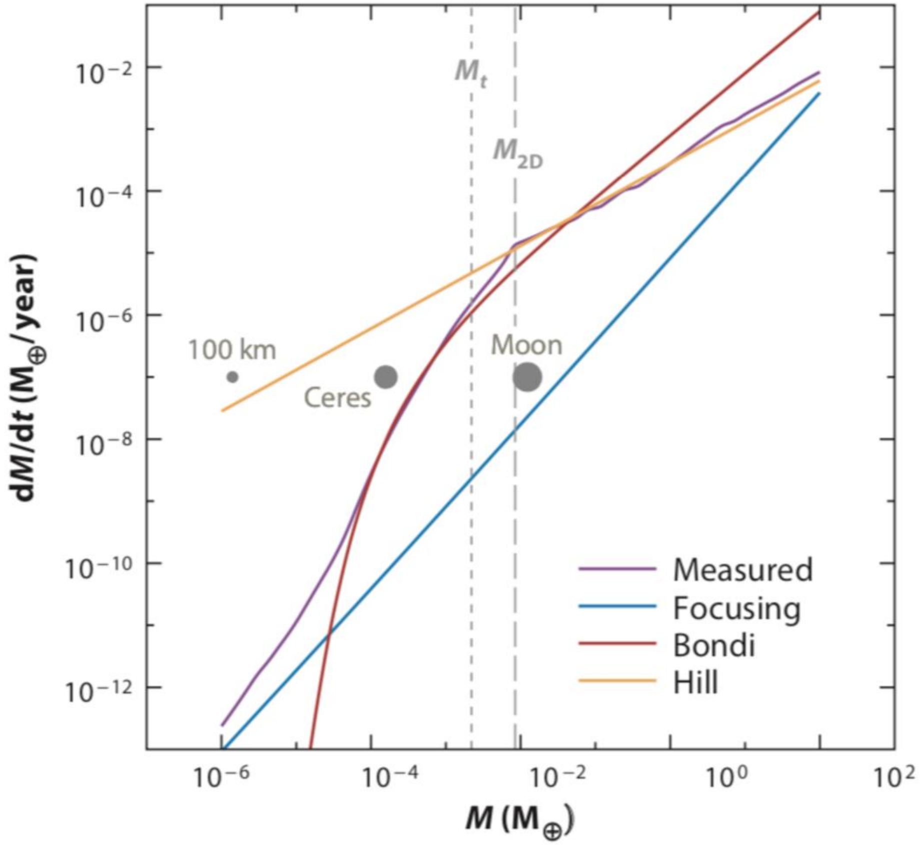

Pebble Accretion: Pebbles of different size accrete differently

Bondi Regime

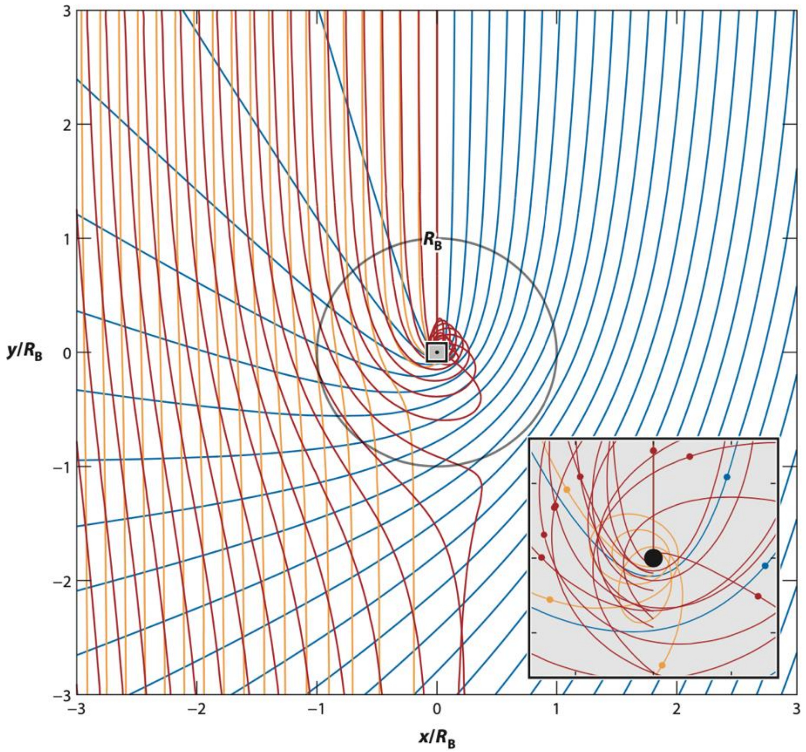

Hill Regime

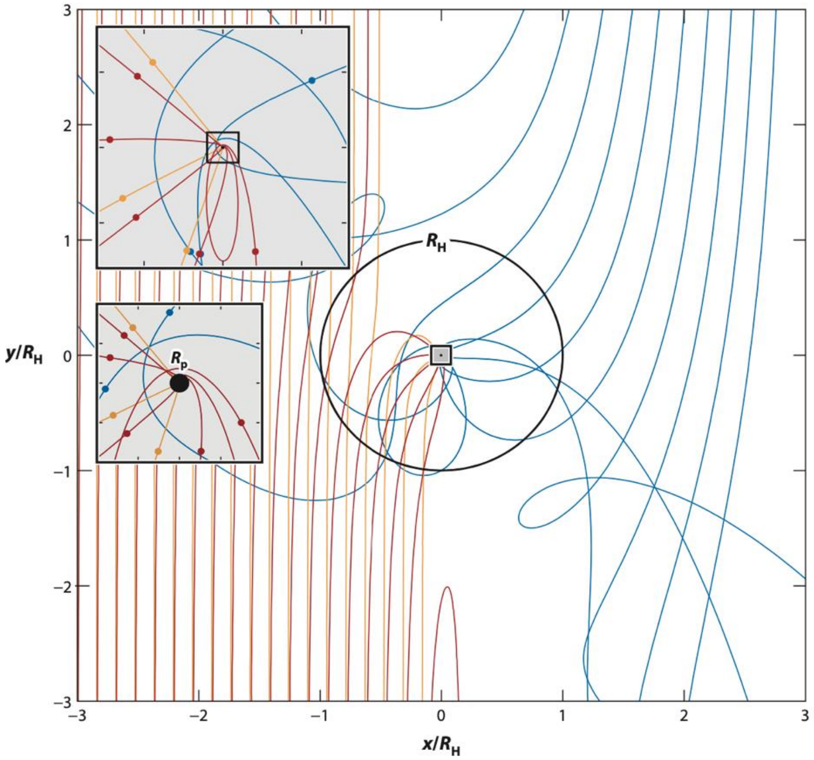

Best accreted pebble

Drag time ~ Bondi Time

Best accreted pebble

Drag time ~ Orbital Time

Johansen & Lambrechts ‘17

Polydisperse (Multi-Species) Pebble Accretion

$$\rho_d(a, z) = \int_0^a m(a')\, F(a', z)\, da'.$$

$$F(a, z) \equiv f(a)\, e^{-z^2/2H_d^2},$$

$$f(a) = \frac{3(1-p)Z\Sigma_g}{2^{5/2}\pi^{3/2}H_g\rho_\bullet^{(0)}a_{\max}^{4-k}}\sqrt{1 + a\frac{\pi}{2}\frac{\rho_\bullet(a)}{\Sigma_g\alpha}}\; a^{-k}.$$

$$S \equiv \frac{1}{\pi R_{\rm acc}^2}\int_{-R_{\rm acc}}^{R_{\rm acc}} 2\sqrt{R_{\rm acc}^2 - z^2}\, \exp\left(-\frac{z^2}{2H_d^2}\right) dz,$$

$$W(a) = \frac{3(1-p)Z\Sigma_g}{4\pi\rho_\bullet^{(0)}a_{\max}^{4-k}}\, a^{-k},$$

$$\delta v \equiv \Delta v + \Omega R_{\rm acc},$$

$$R_{\rm acc} \equiv \hat{R}_{\rm acc}\exp[-\chi(\tau_f/t_p)^\gamma],$$

$$\hat{R}_{\rm acc}^{\rm (Bondi)} = \left(\frac{4\tau_f}{t_{\rm B}}\right)^{1/2} R_{\rm B},$$

$$\hat{R}_{\rm acc}^{\rm (Hill)} = \left(\frac{\rm St}{0.1}\right)^{1/3} R_{\rm H},$$

$$\frac{\partial\Sigma_d(a)}{\partial a} \propto a^{-p};$$

$$\rho_\bullet \propto a^{-q};$$

$$t_p \equiv \frac{GM_p}{(\Delta v + \Omega R_{\rm H})^3}$$

$$\dot{M}(a) = \int_0^a \frac{\partial \dot{M}(a')}{\partial a'}da',$$

$$\frac{\partial \dot{M}(a)}{\partial a} = \pi R_{\rm acc}^2(a)\delta v(a) S(a) m(a) f(a).$$

$$\dot{M}_{\rm 2D,\,Hill} = 2 \times 10^{2/3}\Omega R_H^2 \int_0^{a_{\max}} {\rm St}(a)^{2/3}\, m(a)\, W(a)\, da.$$

$$\dot{M}_{\rm 3D,\,Bondi} = \frac{4\pi R_{\rm B}\Delta v^2}{\Omega} \times \int_0^{a_{\max}} {\rm St}\; e^{-2\psi} m(a) f(a) \times \left[1 + 2\left({\rm St}\frac{\Omega R_{\rm B}}{\Delta v}\right)^{1/2} e^{-\psi}\right] da,$$

$$\psi \equiv \chi[{\rm St}/(\Omega t_p)]^\gamma.$$

Lyra et al. 2023

Analytical theory of polydisperse (multi-species) pebble accretion

Monodisperse (single species)

$$\xi \equiv \left(\frac{R_{\rm acc}}{2H_d}\right)^2$$

$$\dot{M}_{\rm 3D} = \lim_{\xi \to 0} \dot{M} = \pi R_{\rm acc}^2 \rho_{d0} \delta v,$$

$$\dot{M}_{\rm 2D} = \lim_{\xi \to \infty} \dot{M} = 2 R_{\rm acc} \Sigma_d \delta v,$$

Lambrechts & Johansen (2012)

Polydisperse (multiple species)

$$\dot{M}_{\rm 2D,Hill} = \frac{6(1-p)}{14-5q-3k}\left(\frac{\rm St_{max}}{0.1}\right)^{2/3} \Omega R_H^2 Z \Sigma_g.$$

$$\dot{M}_{\rm 3D,Bondi} \approx C_1 \frac{\gamma_l\left(\frac{b_1+1}{s}, j_1 a_{\rm max}^s\right)}{s\, j_1^{(b_1+1)/s}} + C_2 \frac{\gamma_l\left(\frac{b_2+1}{s}, j_2 a_{\rm max}^s\right)}{s\, j_2^{(b_2+1)/s}} + C_3 \frac{\gamma_l\left(\frac{b_3+1}{s}, j_3 a_{\rm max}^s\right)}{s\, j_3^{(b_3+1)/s}} + C_4 \frac{\gamma_l\left(\frac{b_4+1}{s}, j_4 a_{\rm max}^s\right)}{s\, j_4^{(b_4+1)/s}},$$

Lyra et al. (2023)

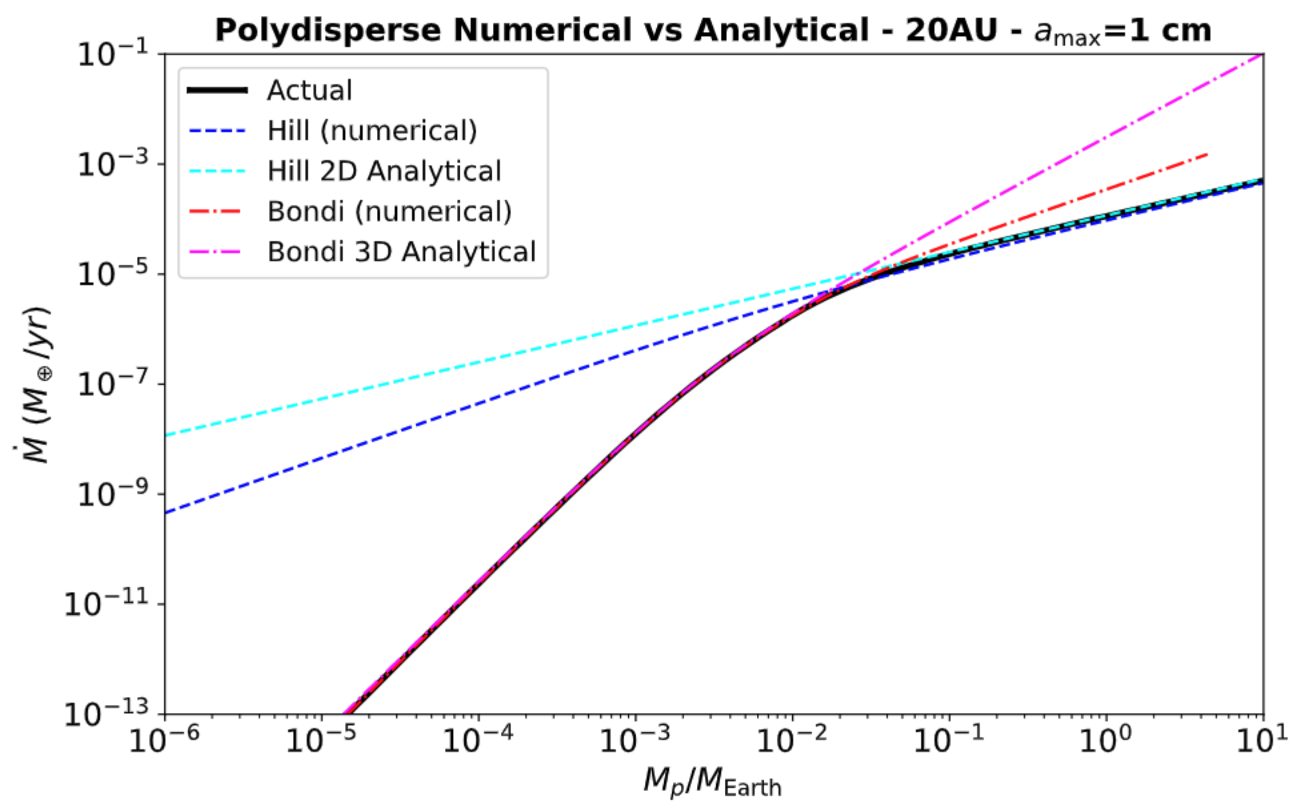

Lyra et al. 2023

Analytical Solution for
General Monodisperse (single species) Pebble Accretion

$$\dot{M} = \pi R_{\rm acc}^2 \rho_{d0}\, S\, \delta v.$$

$$S \equiv \frac{1}{\pi R_{\rm acc}^2} \int_{-R_{\rm acc}}^{R_{\rm acc}} 2\sqrt{R_{\rm acc}^2 - z^2}\, \exp\left(-\frac{z^2}{2H_d^2}\right)\, dz,$$

$$S = e^{-\xi}\left[I_0(\xi) + I_1(\xi)\right], \qquad \xi \equiv \left(\frac{R_{\rm acc}}{2H_d}\right)^2$$

```
y = (x/2)**2

# Modified Bessel function of the first kind of real order.
I0 = sp.special.iv(0, y)
I1 = sp.special.iv(1, y)

Sint = np.exp(-y) * (I0 + I1)
rho_int = rhop * Sint
Mdot = pi*r**2 * rho_int * deltav
```

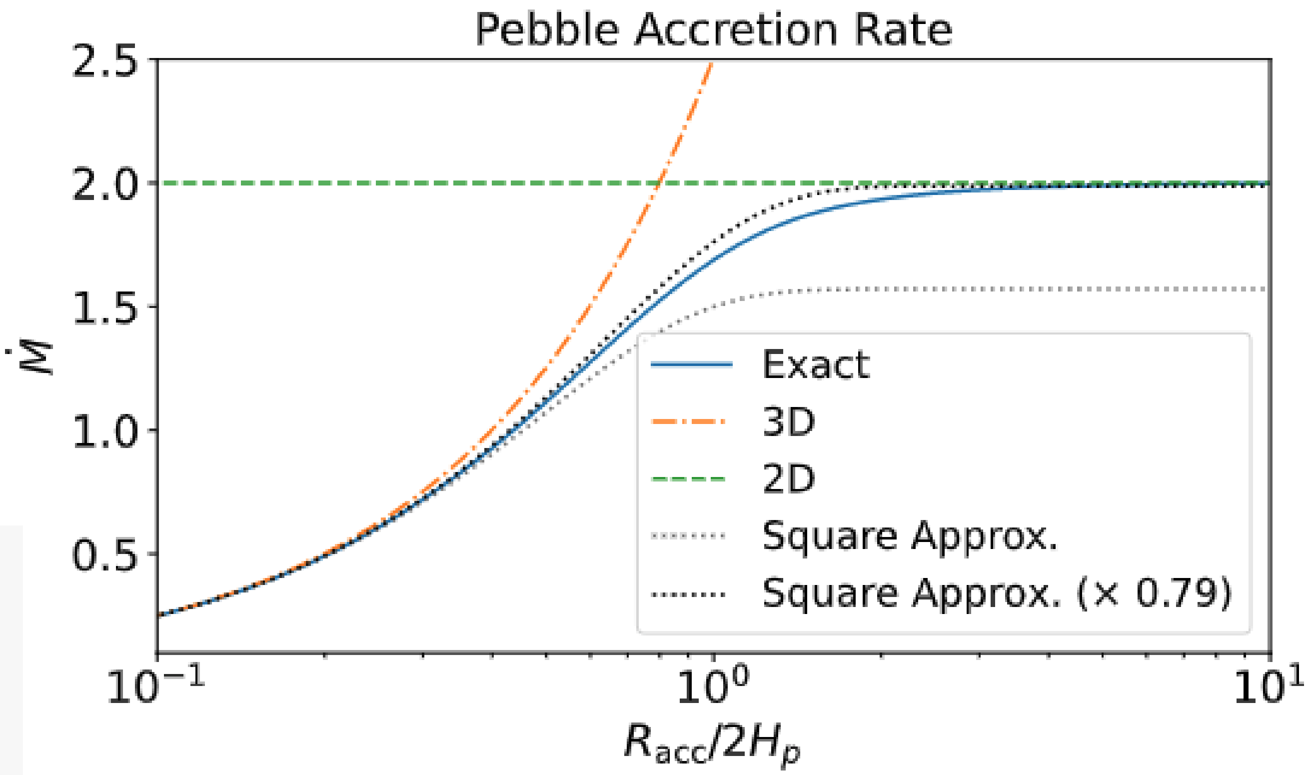

Lyra et al. 2023

Analytical Solutions for
2D and 3D Polydisperse (multi-species) Pebble Accretion

$$\dot{M}_{\rm 2D,Hill} = \frac{6(1-p)}{14-5q-3k}\left(\frac{\rm St_{max}}{0.1}\right)^{2/3}\Omega R_H^2 Z\Sigma_g.$$

$$\dot{M}_{\rm 3D,Bondi} \approx C_1\frac{\gamma_l\left(\frac{b_1+1}{s}, j_1 a^s_{\rm max}\right)}{s\, j_1^{(b_1+1)/s}} + C_2\frac{\gamma_l\left(\frac{b_2+1}{s}, j_2 a^s_{\rm max}\right)}{s\, j_2^{(b_2+1)/s}} + C_3\frac{\gamma_l\left(\frac{b_3+1}{s}, j_3 a^s_{\rm max}\right)}{s\, j_3^{(b_3+1)/s}} + C_4\frac{\gamma_l\left(\frac{b_4+1}{s}, j_4 a^s_{\rm max}\right)}{s\, j_4^{(b_4+1)/s}}$$

```
gamma11 = sp.special.gammainc((b1+1)/s,j1*a**s)*sp.special.gamma((b1+1)/s)
gamma12 = sp.special.gammainc((b2+1)/s,j2*a**s)*sp.special.gamma((b2+1)/s)
gamma13 = sp.special.gammainc((b3+1)/s,j3*a**s)*sp.special.gamma((b3+1)/s)
gamma14 = sp.special.gammainc((b4+1)/s,j4*a**s)*sp.special.gamma((b4+1)/s)

G1 = C1*gamma11/s/j1**((b1+1)/s)
G2 = C2*gamma12/s/j2**((b2+1)/s)
G3 = C3*gamma13/s/j3**((b3+1)/s)
G4 = C4*gamma14/s/j4**((b4+1)/s)

Mbondi3d = G1 + G2 + G3 + G4
```

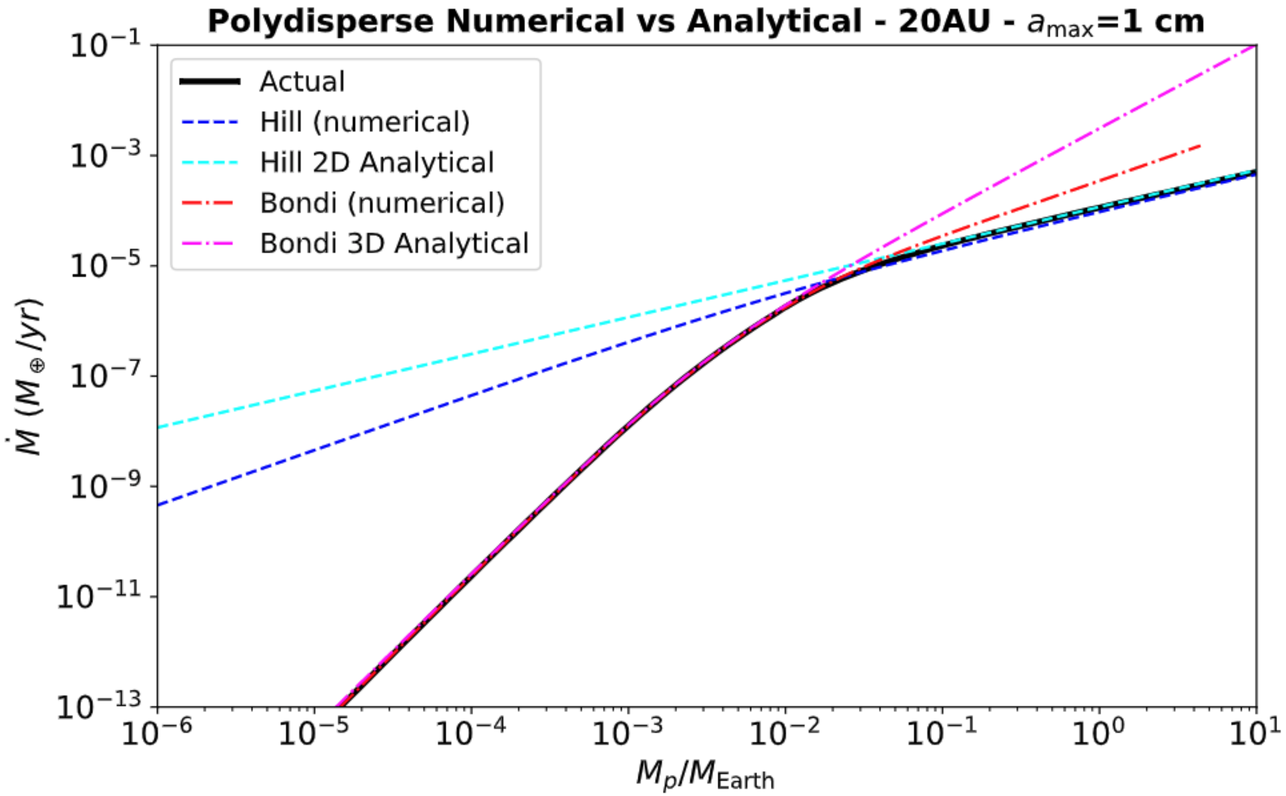

Lyra et al. 2023

Accretion Rates

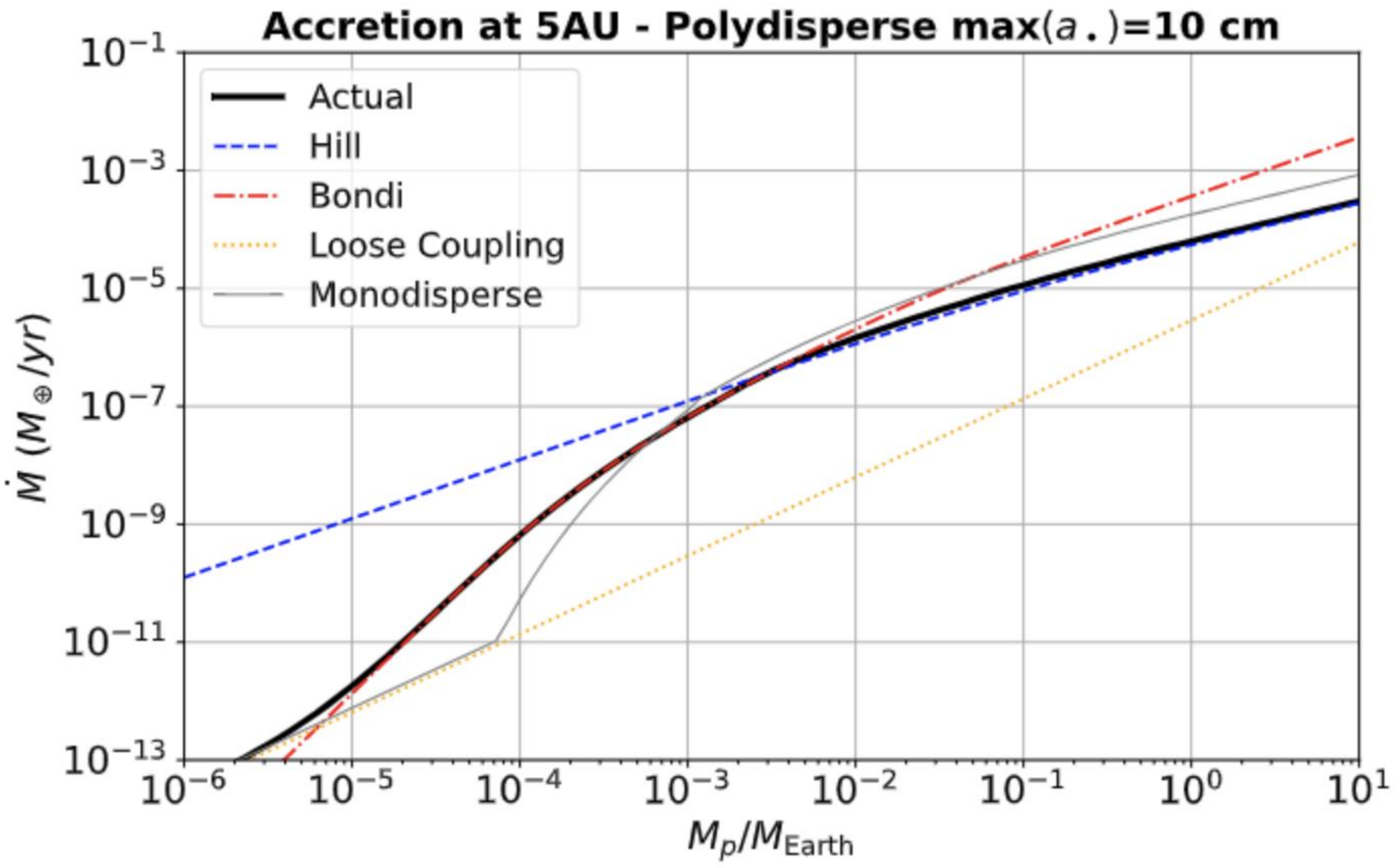

Lyra et al. 2023

Accretion Rates

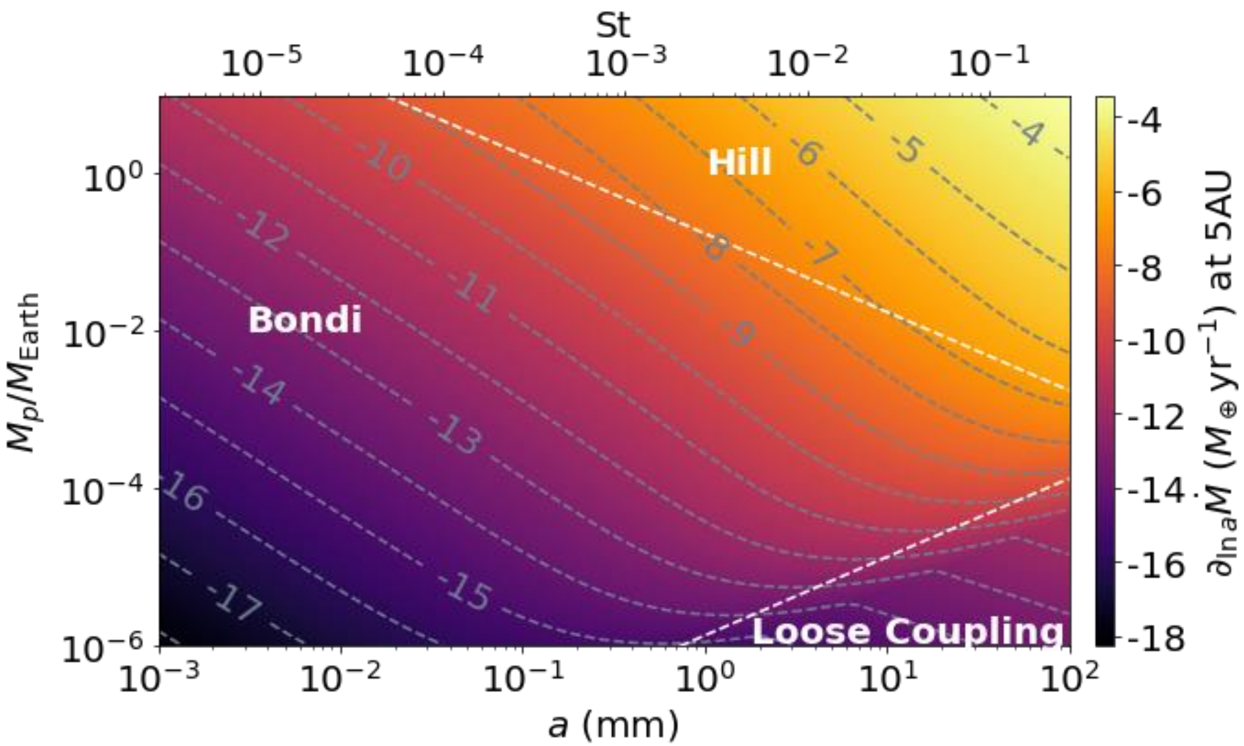

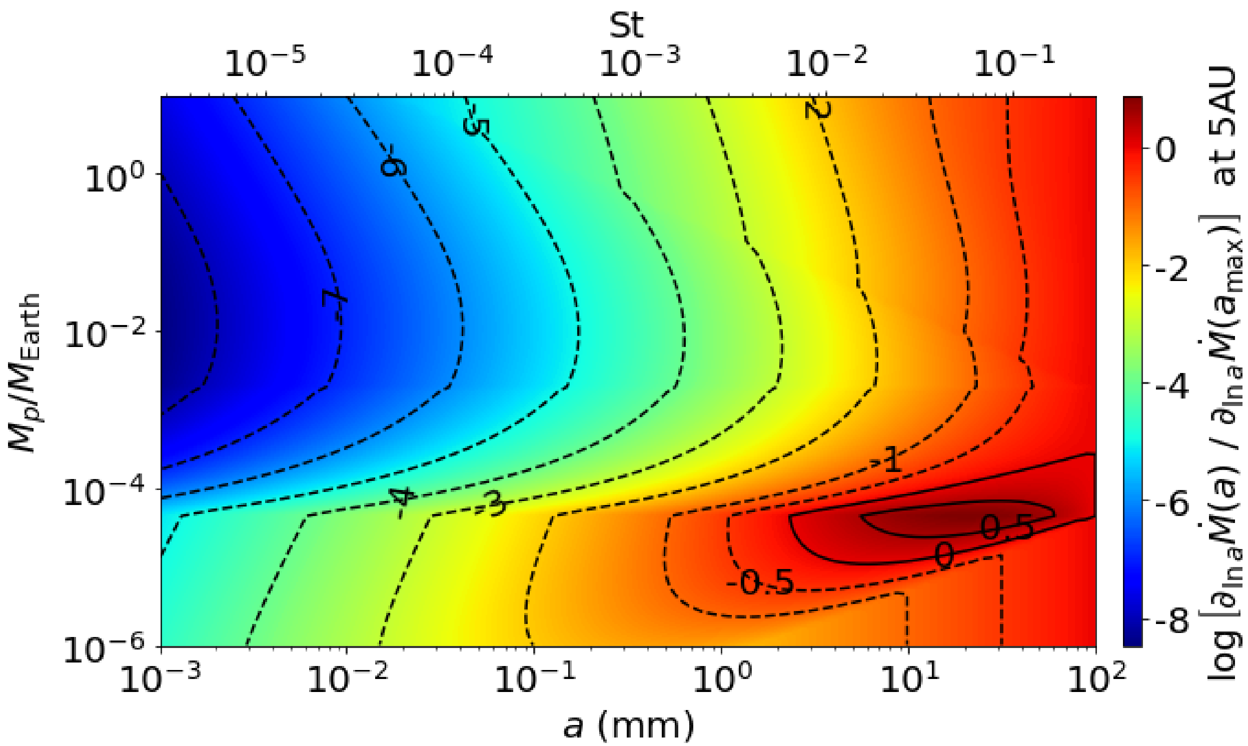

Lyra et al. 2023

Accretion Timescales

Myr accretion timescales possible on top of planetesimals produces by Streaming Instability

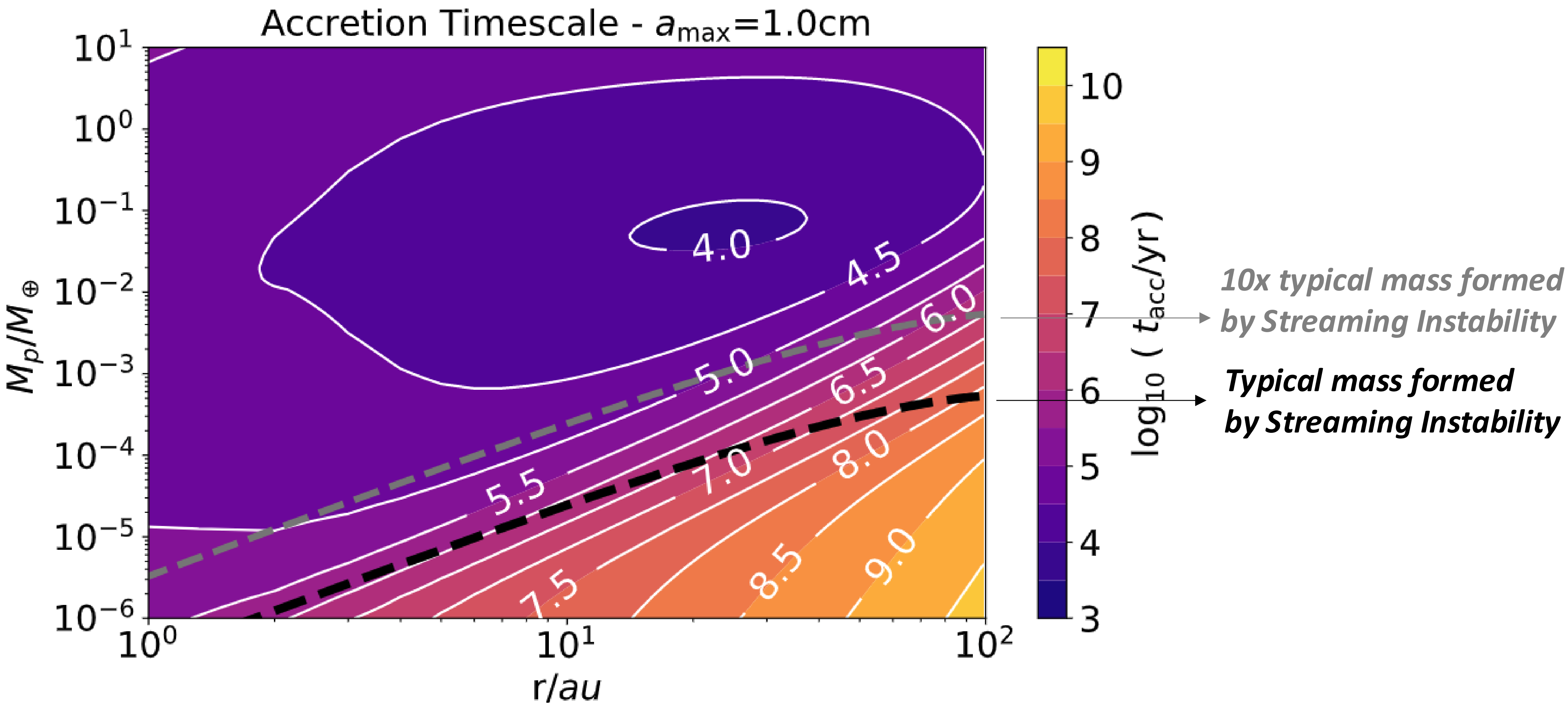

Lyra et al. 2023

Growing Pluto by silicate pebble accretion

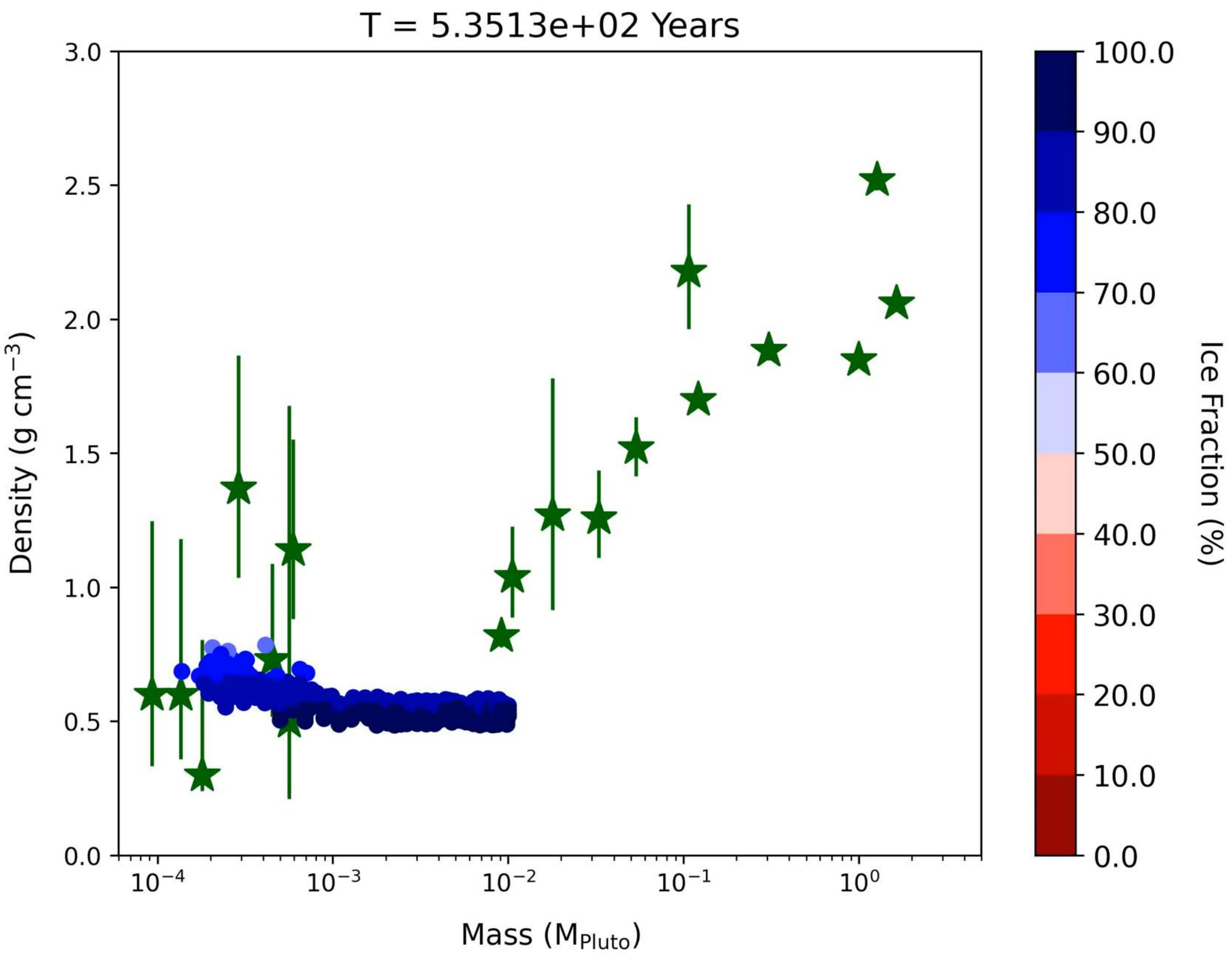

Canas+Lyra et al. 2024

Pebble Internal Density

Ice Volume Fraction

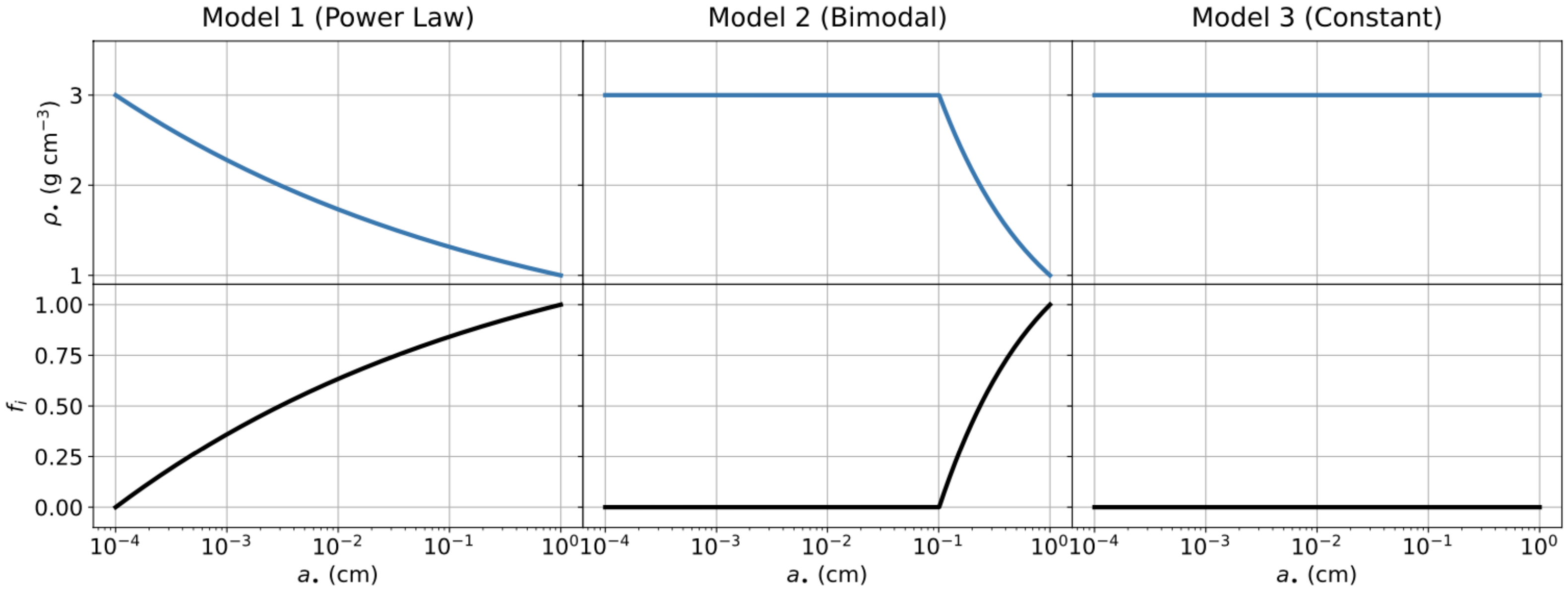

Mass Accretion rate

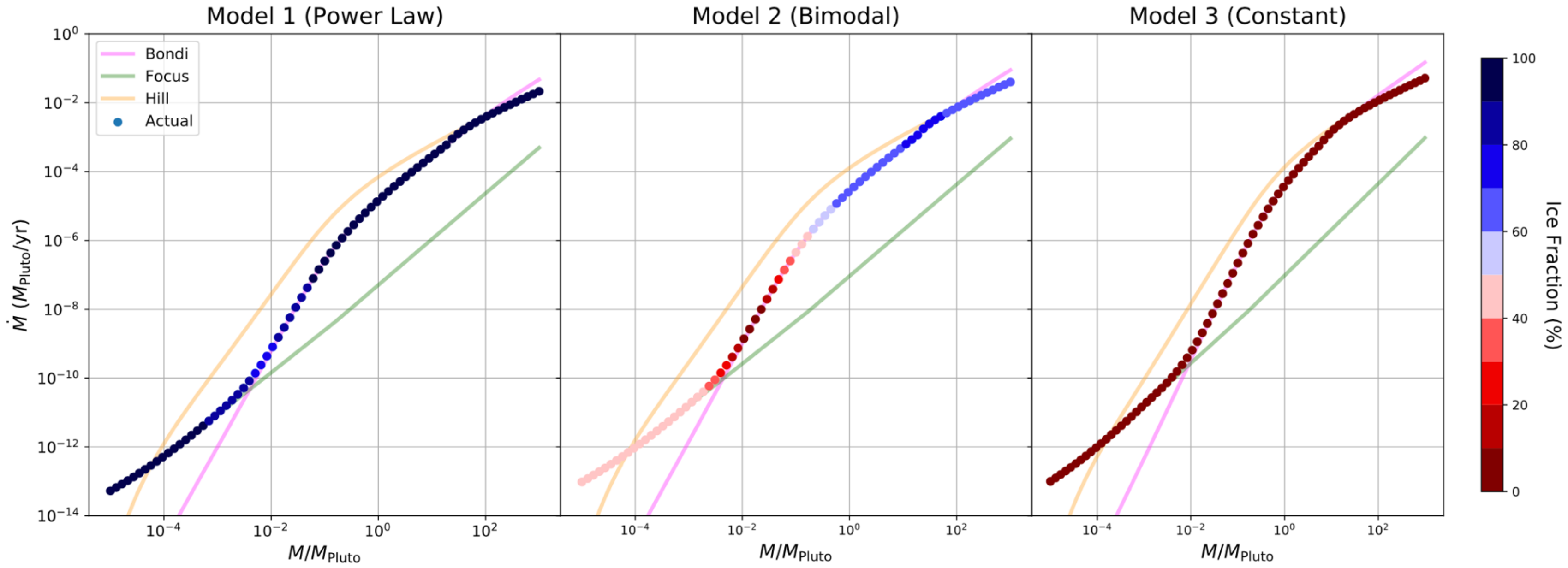

Canas+Lyra et al. 2024

Growing Pluto by silicate pebble accretion

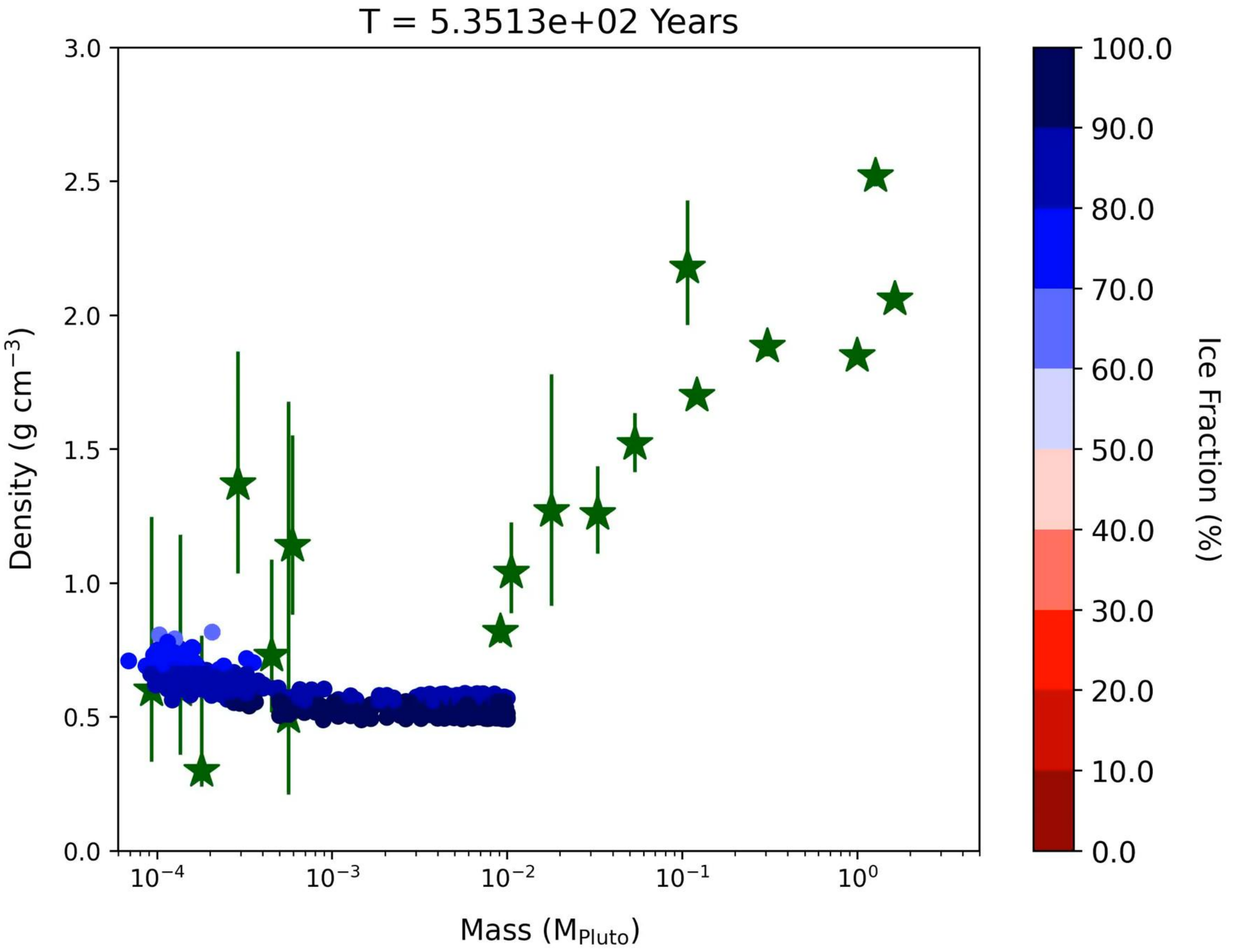

Canas+Lyra et al. 2024

Resulting Densities vs Mass relations

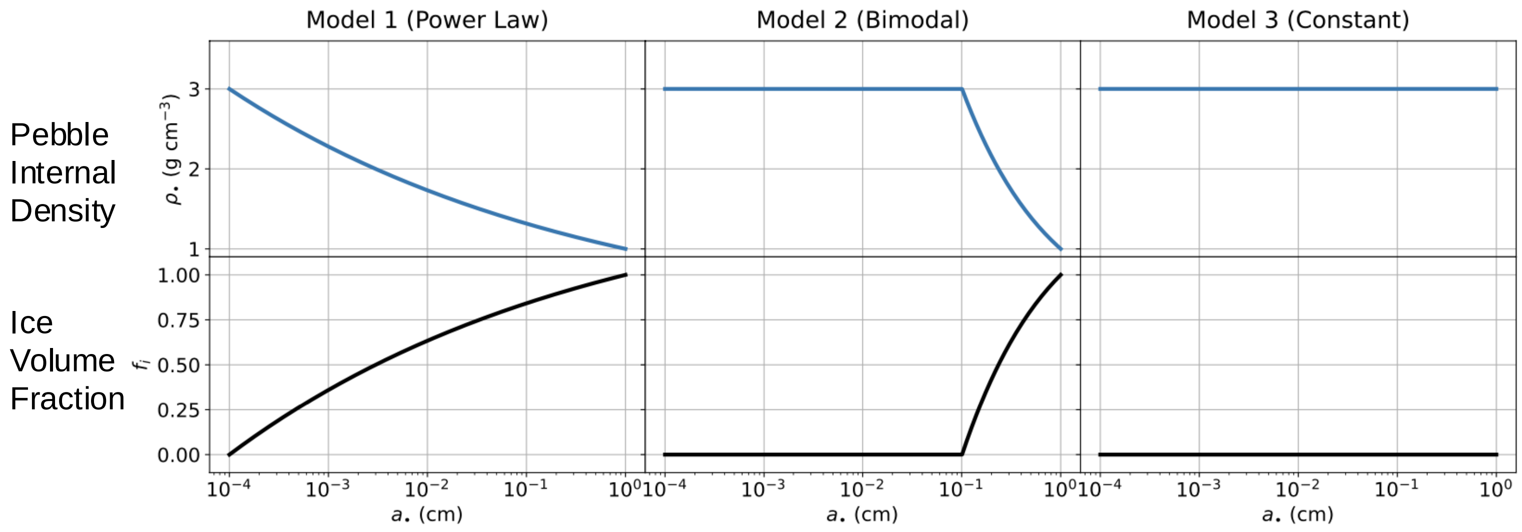

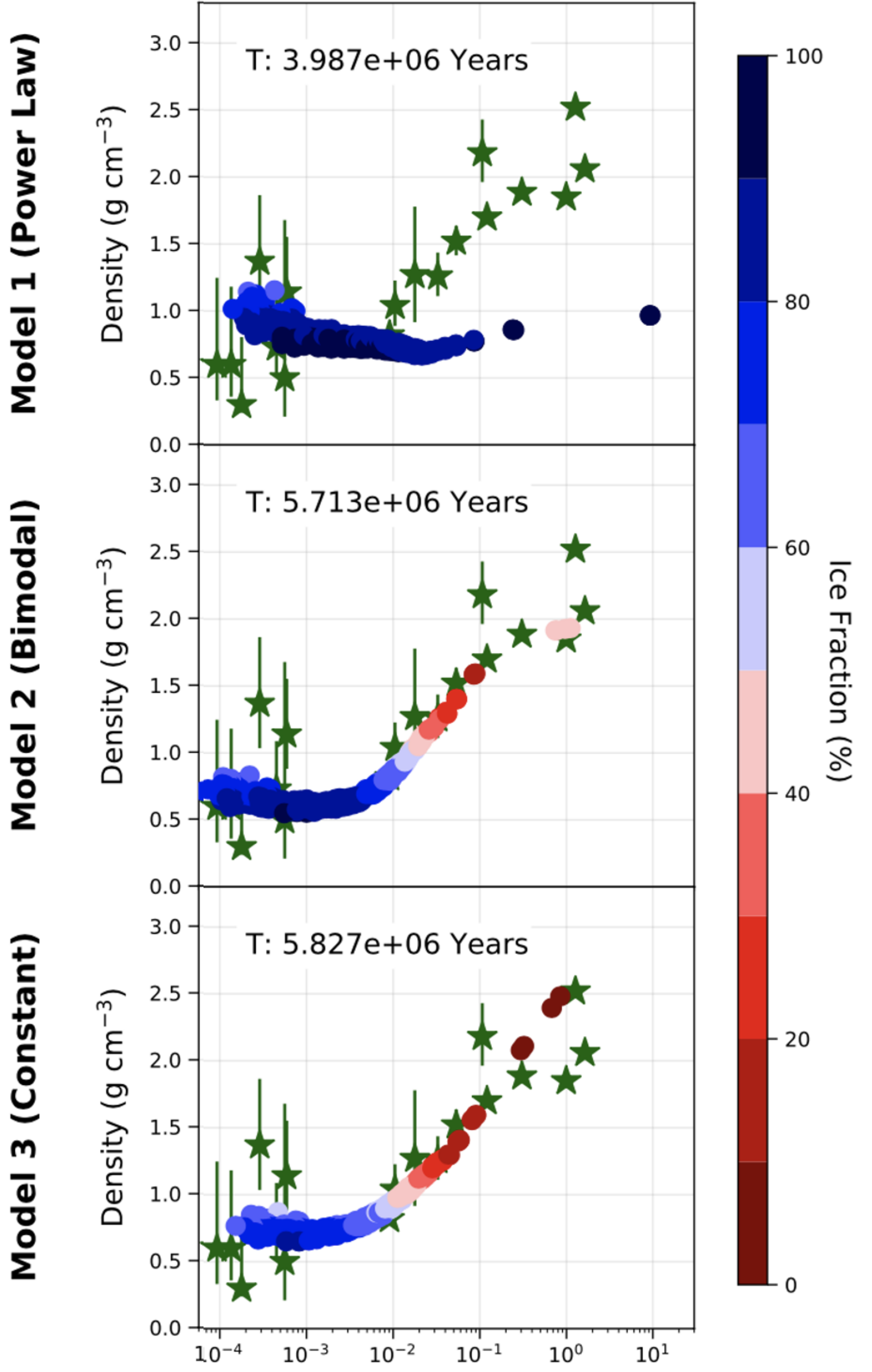

Canas+Lyra et al. 2024

Distance Range
15 - 25AU

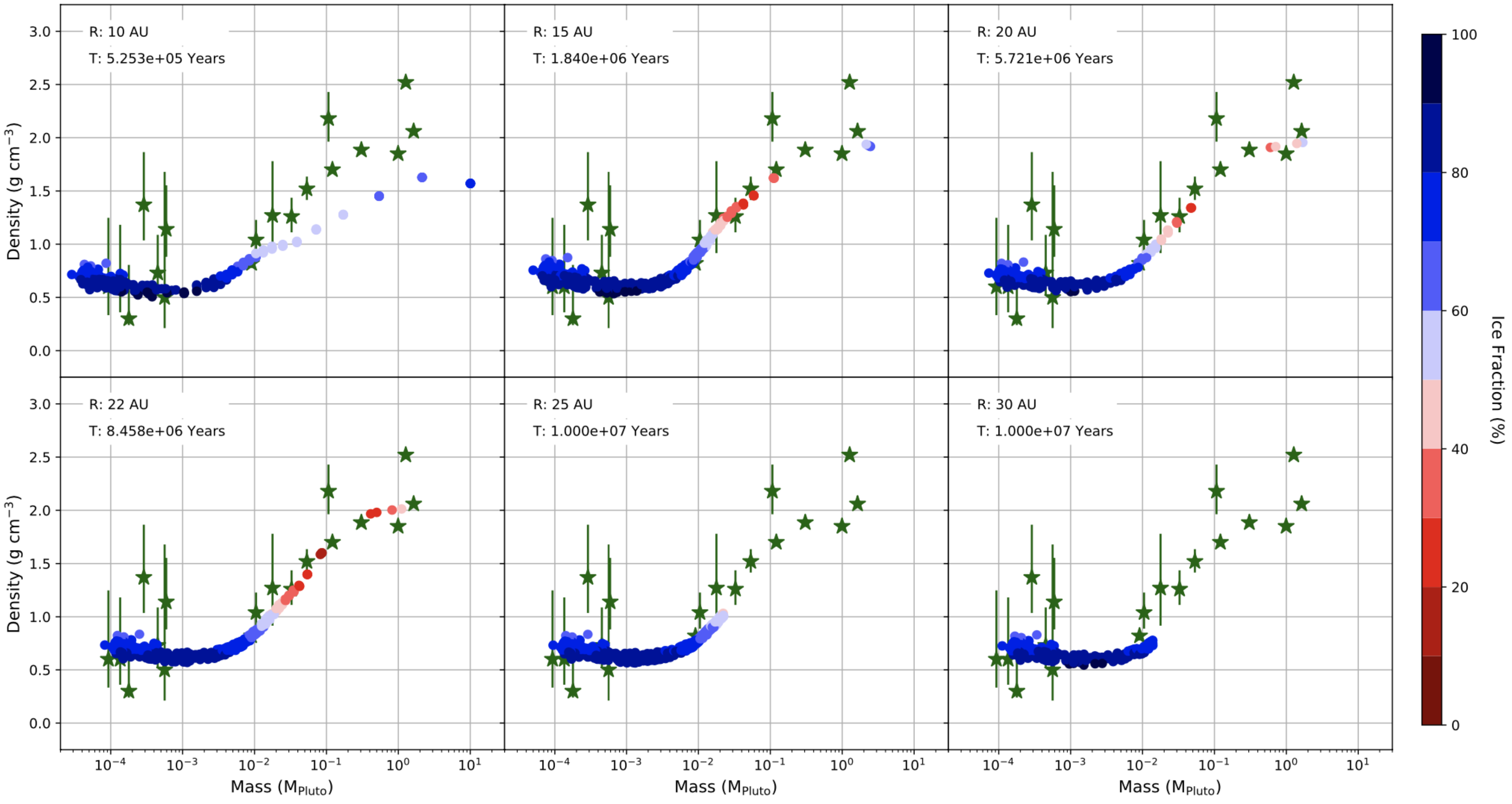

Canas+Lyra et al. 2024

The window of silicate accretion

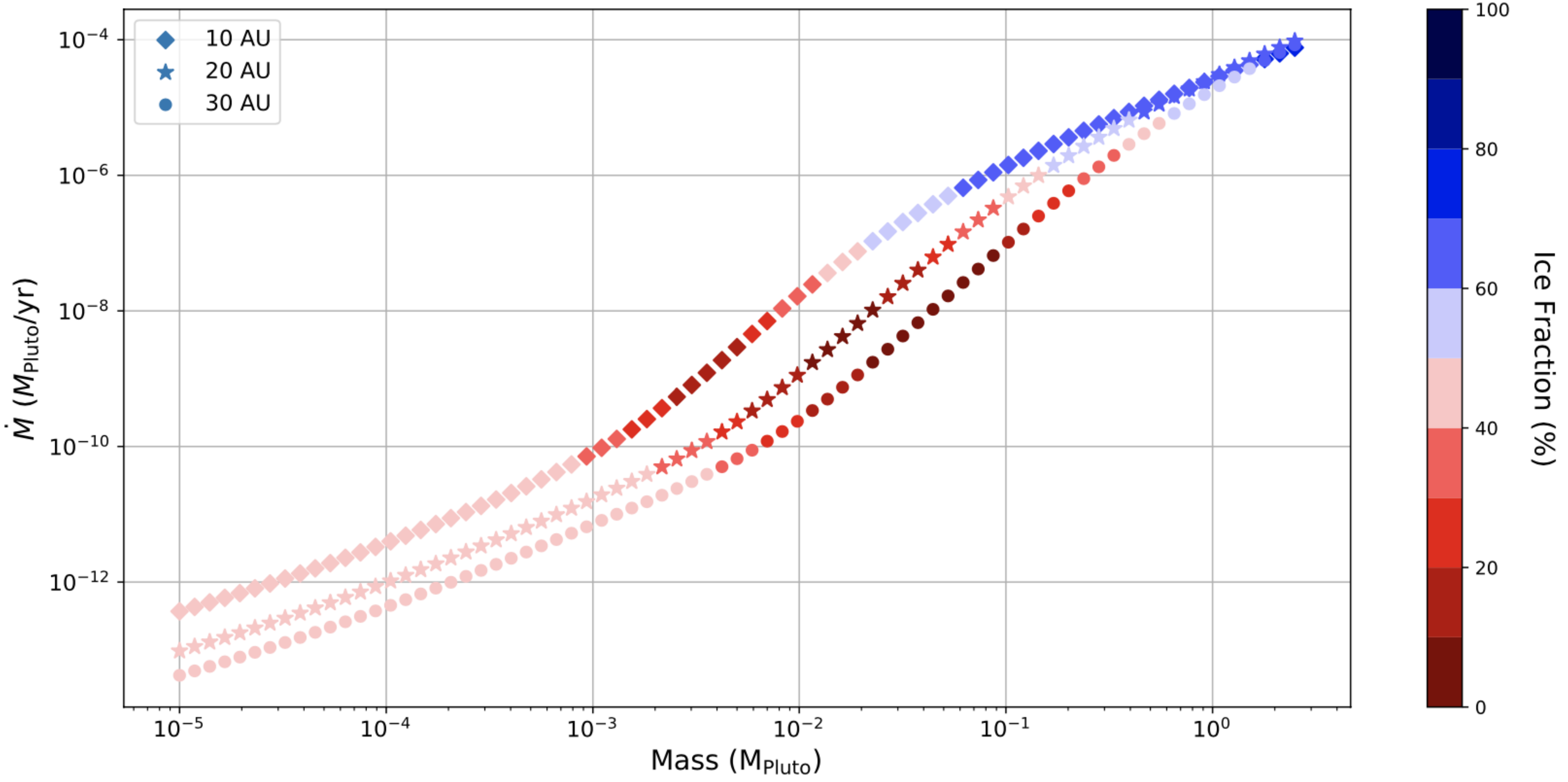

Canas+Lyra et al. 2024

Conclusions

- Polydisperse Bondi accretion 1-2 orders of magnitude more efficient than monodisperse
  - Best accreted pebbles are those of drag time ~ Bondi time, not the largest ones
  - The largest ones dominate the mass budget, but accrete poorly
- Onset of Bondi accretion 1-2 orders of magnitude lower in mass compared to monodisperse
  - Bondi accretion possible on top of Streaming Instability planetary embryos within disk lifetime
  - Reaches 100-350km objects within Myr timescales
- Analytical solution to
  - Monodisperse general case
  - Polydisperse 2D Hill and 3D Bondi
- KBO density problem:
  - Two different pebble populations, maintained by ice desorption off small grains
  - Streaming instability: icy-rich small objects; nearly uniform composition
  - Polydisperse pebble accretion: silicate-rich larger objects; varied composition
  - Melting avoided by
    - ice-rich formation
    - ^{26}Al incorporated mostly in long (>Myr) phase of silicate accretion
  - KBOs best reproduced between 15-25 AU

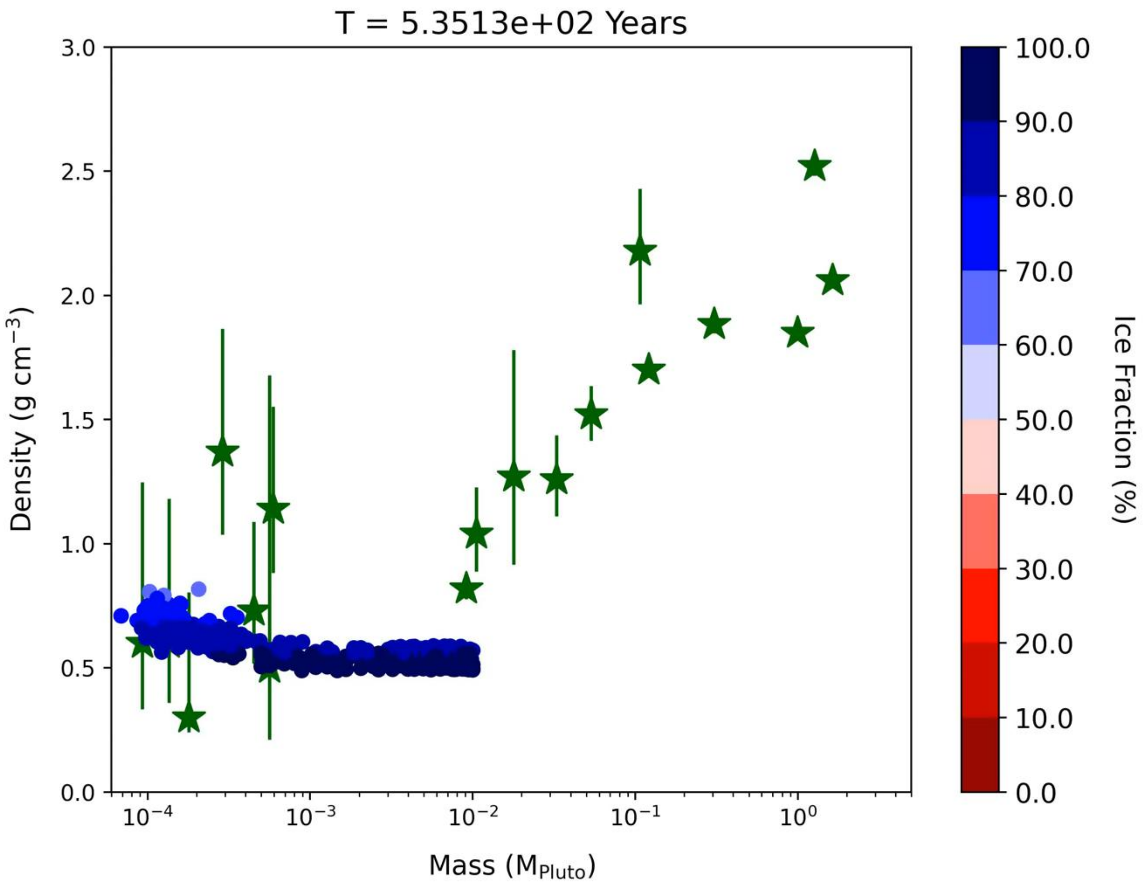

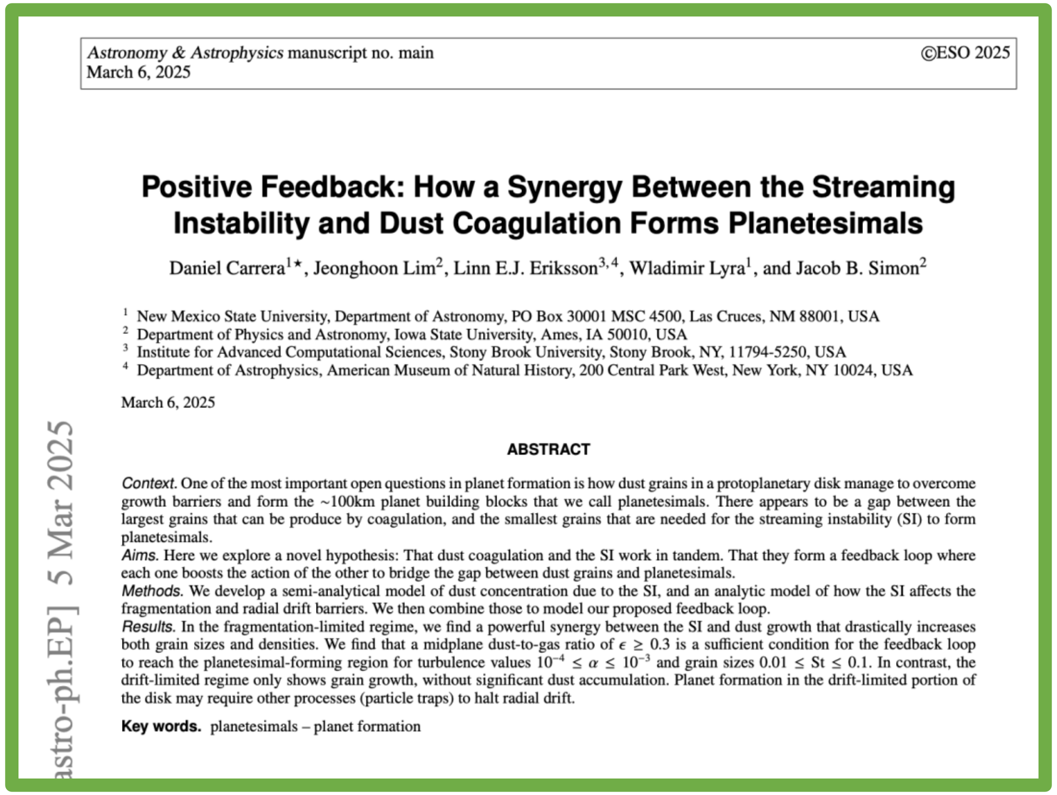

Astronomy & Astrophysics manuscript no. main ©ESO 2025
March 6, 2025

Positive Feedback: How a Synergy Between the Streaming Instability and Dust Coagulation Forms Planetesimals

Daniel Carrera[1⋆], Jeonghoon Lim[2], Linn E.J. Eriksson[3,4], Wladimir Lyra[1], and Jacob B. Simon[2]

[1] New Mexico State University, Department of Astronomy, PO Box 30001 MSC 4500, Las Cruces, NM 88001, USA
[2] Department of Physics and Astronomy, Iowa State University, Ames, IA 50010, USA
[3] Institute for Advanced Computational Sciences, Stony Brook University, Stony Brook, NY, 11794-5250, USA
[4] Department of Astrophysics, American Museum of Natural History, 200 Central Park West, New York, NY 10024, USA

March 6, 2025

ABSTRACT

Context. One of the most important open questions in planet formation is how dust grains in a protoplanetary disk manage to overcome growth barriers and form the ~100km planet building blocks that we call planetesimals. There appears to be a gap between the largest grains that can be produce by coagulation, and the smallest grains that are needed for the streaming instability (SI) to form planetesimals.
Aims. Here we explore a novel hypothesis: That dust coagulation and the SI work in tandem. That they form a feedback loop where each one boosts the action of the other to bridge the gap between dust grains and planetesimals.
Methods. We develop a semi-analytical model of dust concentration due to the SI, and an analytic model of how the SI affects the fragmentation and radial drift barriers. We then combine those to model our proposed feedback loop.
Results. In the fragmentation-limited regime, we find a powerful synergy between the SI and dust growth that drastically increases both grain sizes and densities. We find that a midplane dust-to-gas ratio of $\epsilon \geq 0.3$ is a sufficient condition for the feedback loop to reach the planetesimal-forming region for turbulence values $10^{-4} \leq \alpha \leq 10^{-3}$ and grain sizes $0.01 \leq \mathrm{St} \leq 0.1$. In contrast, the drift-limited regime only shows grain growth, without significant dust accumulation. Planet formation in the drift-limited portion of the disk may require other processes (particle traps) to halt radial drift.

Key words. planetesimals – planet formation

Daniel Carrera
NMSU

Jeonghoon Lim
ISU

Linn Eriksson
AMNH

Wlad Lyra
NMSU

Jake Simon
ISU

Positive Feedback — A Synergy Between the SI and Dust Coagulation

Motivation: The SI only forms planetesimals if

- Grains are larger than dust models predict, AND/OR
- Z is larger than dust models predict.

Our proposal: A **feedback loop** between the SI and dust coagulation

- The SI creates the conditions for better dust growth.
- Dust growth creates the conditions for better SI.

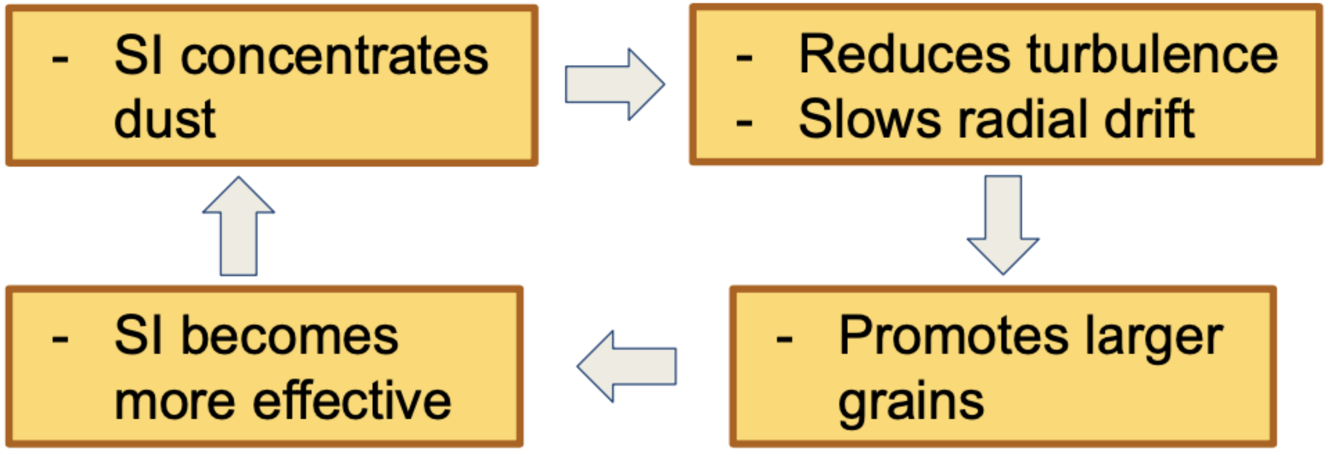

Slide by D. Carrera
Carrera et al. 2025

Positive Feedback — A Synergy Between the SI and Dust Coagulation

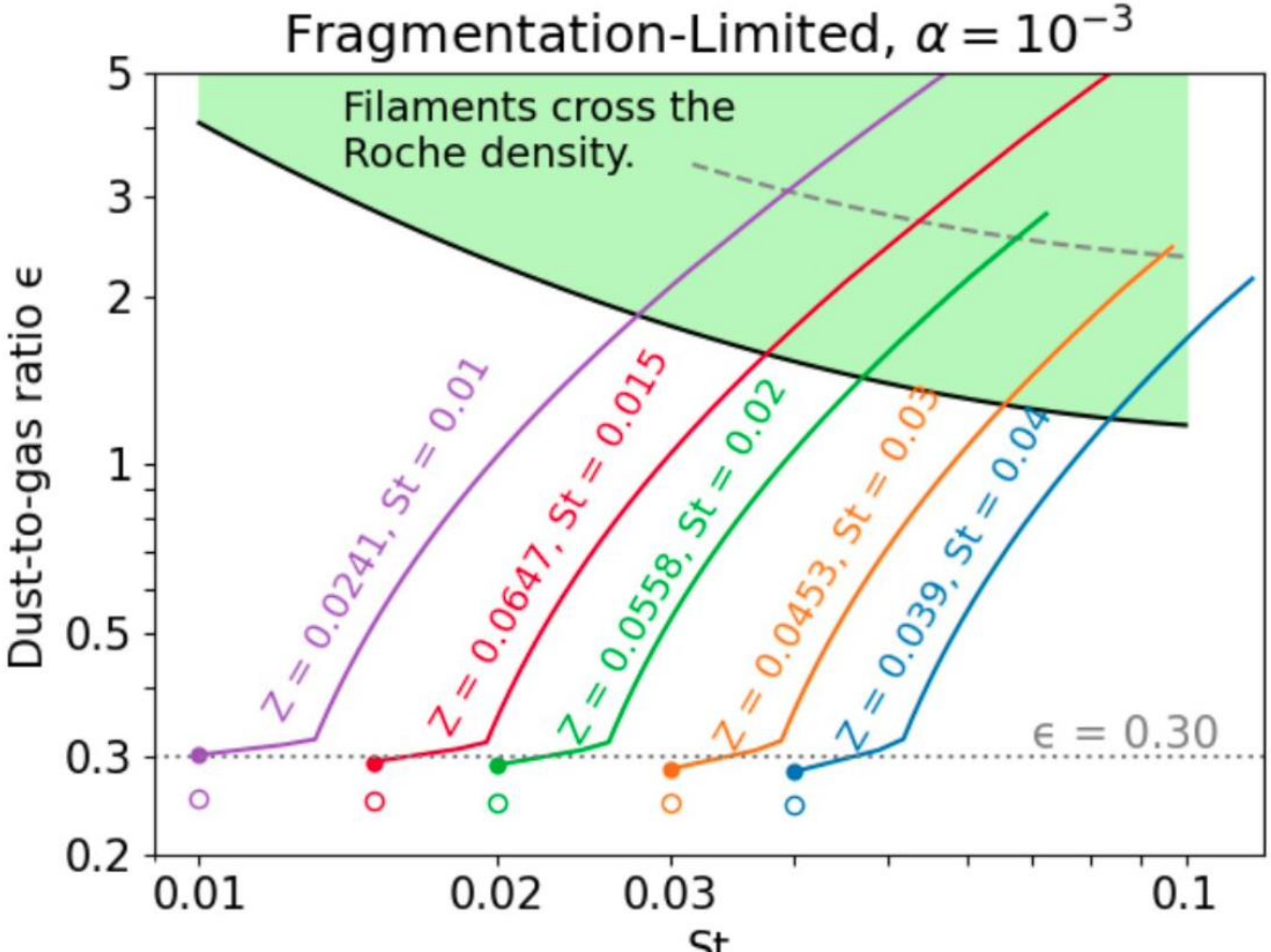

Slide by D. Carrera
Carrera et al. 2025

Summary

Positive Feedback: How a Synergy Between the Streaming Instability and Dust Coagulation Forms Planetesimals

- **Feedback loop** between the SI + dust coagulation largely overcomes the fragmentation barrier

Slide by D. Carrera
Carrera et al. 2025